Universidad de Valladolid

Facultad de Ciencias

Departamento de Física de la Materia Condensada, Cristalografía y Mineralogía

SYNTHESIS AND CHARACTERIZATION OF A SILK-ELASTIN-LIKE RECOMBINAMER FUSED TO ENHANCED GREEN FLUORESCENT PROTEIN (SELR-EGFP) FOR THE ACHIEVEMENT OF SELF-ASSEMBLED FLUORESCENT NANOPARTICLES AND PHYSICALLY CROSS-LINKED HYDROGELS

A Master Thesis for the Degree of M.Sc. Molecular Nanoscience and Nanotechnology presented by

Arturo Ibáñez Fonseca

Supervised by

Prof. Dr. José Carlos Rodríguez Cabello

AGRADECIMIENTOS

En primer lugar, agradecer a mi director de este TFM, Carlos, por dirigir mi trabajo y por darme la oportunidad de adentrarme en los entresijos de la ciencia y, más concretamente, de los recombinámeros de tipo elastina. Asimismo, he de dar las gracias al resto de "seniors" del G.I.R. Bioforge, por su constante apoyo y, en algunos casos, dirección, empezando por Javier Arias, que, indudablemente, ha colaborado a que este trabajo llegue a buen puerto. También a Matilde, Merche, Luis, y Alessandra, que tanto me ayudó en mis inicios y aún hoy sigue aportándome enseñanzas.

También a mis compañeros, a todos ellos, por aportar un ambiente de trabajo agradable y ameno, además de ser fuente de soluciones a todas aquellas dificultades que surgen durante el día a día.

No quiero olvidarme de la profesora María Luz Rodríguez Méndez, coordinadora del máster en la Universidad de Valladolid, que siempre me ha dado facilidades a lo largo del mismo para poder compaginarlo adecuadamente con la tarea investigadora.

Y, sin duda, un especial agradecimiento se merecen las personas que me han apoyado desde fuera, empezando por los amigos, que en momentos de dificultad me han ayudado a sobreponerme, pasando por la familia, que ha sido un apoyo en todo momento, y terminando por María, que tanto ha soportado cuando sobrevenían adversidades.

A todos, gracias.

"Life's but a walking shadow, a poor player

That struts and frets his hour upon the stage

And then is heard no more: it is a tale

Told by an idiot, full of sound and fury,

Signifying nothing."

William Shakespeare. *Macbeth.*

CONTENTS

ABSTRACT

Nanoscience and nanotechnology constitute a combination of knowledge and tools very powerful in the fields of chemistry, physics and biology. The application of these tools in different experimentation areas has allowed, in the last few years, multiple technological progresses already available for final users.

Future perspectives make us anticipate that nanotechnology is going to be even more involved in the development of new biomedical devices for its clinical use. In this subject we can find elastin-like recombinamers (ELRs), of which self-assembly properties in response to different stimuli such us temperature let them to be classified as nanoscience based nanotechnological tools. Briefly, this self-assembly property, related to protein folding, takes place when temperature is raised above what is called transition temperature (Tt), specific for each designed ELR, triggering a phase transition from soluble to non-soluble in an aqueous solution, due to destabilization of water clathrates surrounding hydrophobic residues of the ELR and the hydrophobic interactions between them.

Previous works have given us evidence of the ability of some amphiphilic ELRs to form either nanoparticles (micelles) or hydrogels, depending on the recombinamer concentration (high or low, respectively). These hydrogels are a very promising tool in biomedicine due to its capability of simulate extracellular matrix (ECM), being extremely biocompatible. Furthermore, the combination of these recombinamers with motifs from *Bombyx mori* silk (referred to as silk domains) has reported and improvement of the mechanical properties and the stabilization of the structured hydrogels.

In addition, its recombinant characteristic permits the fusion of other proteins or peptides to an SELR backbone able to self-assemble, by the usage of recombinant DNA technology with the aim of obtaining fusion recombinamers with different bioactivities.

In this work, the protein fused to an SELR backbone is the Enhanced Green Fluorescent Protein (EGFP) in order to obtain different florescent nanostructures such us micelle-like nanoparticles or hydrogels, depending on the SELR concentration, as

described above. These hydrogels, combined with other hydrogel forming SELRs with other bioactivities, could lead, when implanted, to the tracking of the material throughout the body with different fluorescence *in vivo* imaging devices.

It is also part of the work the characterization of the designed SELR, taking into account its protein composition, as well as *in vitro* experiments in cell cultures of micro and nanoparticles obtained by an approach of Layer by Layer (LbL) technique with the combination of two different SELRs with positively and negatively charged groups, being one of them the recombinamer presented in this work, named $(EIS)_2$-EGFP or, simply, SELR-EGFP, allowing the observation of these particles in cell cultures by fluorescence microscopy.

RESUMEN

La nanociencia y la nanotecnología constituyen un conjunto de conocimientos y herramientas muy poderosas en el ámbito de la química, la física y la biología. La aplicación de estas herramientas en los distintos campos de experimentación ha permitido, en los últimos años, múltiples avances tecnológicos disponibles para el usuario final.

Las perspectivas de futuro nos hacen prever que la nanotecnología estará aún más implicada de lo que ya lo está en la fabricación de dispositivos biomédicos para su uso en clínica. Dentro de este apartado se encuentran los recombinámeros de tipo elastina (ELRs, en inglés), cuya propiedad de auto-ensamblado en respuesta a estímulos como la temperatura permite enmarcarlos dentro de la nanociencia y la nanotecnología. Brevemente, su característica principal es el plegamiento o self-assembly cuando la temperatura es superior a la que se denomina temperatura de transición (T_t), lo que conlleva una transición de soluble a insoluble en un disolvente acuoso, debido a la ruptura de las jaulas de clatrato y a las interacciones hidrofóbicas.

Estudios previos han demostrado la capacidad de algunos ELRs anfifílicos de formar bien micelas o bien hidrogeles, en función de la concentración de recombinámero (baja o alta, respectivamente). Estos hidrogeles son una herramienta con un elevado potencial en biomedicina por su capacidad de simular la matriz extracelular, siendo extremadamente biocompatible. Además, la adición de secuencias de aminoácidos provenientes de la secuencia de la seda de *Bombyx mori* ha demostrado mejorar tanto las propiedades mecánicas como la estabilidad de los hidrogeles.

También, su característica recombinante permite la fusión de otras proteínas presentes en la naturaleza mediante la tecnología de ADN recombinante, con el objetivo de obtener polímeros de fusión que, además de proporcionar un esqueleto para el desarrollo de matrices, tengan diferentes bioactividades.

En este trabajo, se ha utilizado como proteína de fusión la proteína verde fluorescente mejorada (Enhanced Green Fluorescent Protein, EGFP), con el objetivo de desarrollar nanoestructuras tipo nanopartículas e hidrogeles fluorescentes. Este material, combinado con otros materiales capaces de formar hidrogeles, que aportasen

distintas bioactividades, permitiría, una vez implantado, monitorizar, mediante distintos dispositivos de visualización de fluorescencia *in vivo*, el tránsito del hidrogel por el organismo en el cual se ha implantado.

Se presenta, además, la caracterización completa del material teniendo en cuenta su carácter proteico, así como experimentos *in vitro* en cultivos celulares de micro y nanopartículas obtenidas por Layer by Layer (LbL) mediante la combinación de dos ELRs distintos con grupos funcionales cargados positiva y negativamente, siendo uno de ellos el recombinámero objeto de estudio en este trabajo denominado $(EIS)_2$-EGFP o, simplemente, SELR-EGFP, lo que permite su observación en el cultivo celular mediante microscopía de fluorescencia.

1. INTRODUCTION

1.1 Introduction to nanoscience and nanotechnology

Nanoscience is the study of phenomena at nanometre scale in many research fields, like physics (e.g. quantum effects), chemistry (e.g. study of supramolecular structures like micelles) and biology (e.g. investigation of DNA, proteins and other biomolecules assembling). The knowledge and the improvements derived from nanoscience can be applied to the development of tools, which make up nanotechnology. As the properties of materials in the nano scale are completely different from the ones in bulk size, new applications arise from nanotechnology.

The development of nanotechnological tools can be achieved by two different approaches:

- Top-down: this approach consist in obtaining very small structures from larger ones by different techniques, such as photolithography, but has drastic limitations for getting objects of dimensions smaller than 100nm.
- Bottom-up: in this approach, small molecules are used to build up supramolecular nanostructures, by the use of methods like layer by layer, colloid formation and others related to polymer science, for example. In this work, this approach will be used to obtain nanoparticles (NPs) by the aggregation of an amphiphilic protein polymer in a self-assembling process and later to get larger NPs by the combination of two different polymers with a layer by layer approach.

1.2 Protein based materials

Protein based-materials have drawn attention of numerous researchers in recent years as promising advanced biomaterials for use in the field of biomedicine, especially as a result of recent improvements in recombinant DNA technology, which allow us to design and manufacture materials by exploiting the abilities of natural proteins [1]. Some of the most widely studied protein-derived materials are the so-called elastin like recombinamers (ELRs) [2-4], taking into account its recombinant

nature this new nomenclature was proposed [5] in replacement of the more conventional terminology elastin-like polymers (ELPs), which include those first chemically synthesized materials.

1.2.1   *Elastin-like recombinamers (ELRs)*

ELRs are smart, genetically engineered biomaterials inspired by natural elastin and based on the very same recurring amino acid sequences as an ability to undergo high deformation without breaking and subsequent recovery of the original conformation once the stress disappears [6, 7]. The origin of this ability resides in the structure of the recurrent sequences (VPGVG, VPGG, VGVAPG) found in tropoelastin [8]. Some of the most relevant characteristics of ELRs, which are derived from those of the natural protein, serve as an example of how elastin's mechanical properties are retained by way of cross-linked ELR matrices [9]. These mechanical properties become more interesting in conjunction with other properties such as biocompatibility, stimuli-responsive behavior and the ability to self-assemble [10, 11]. The most widely studied ELRs are based on the recurring pentapeptide sequence Val-Pro-Gly-Xaa-Gly, where Xaa is any natural amino acid except proline.

1.2.1.1 *Inverse temperature transition (ITT)*

All functional ELRs present a reversible phase transition in response to changes in temperature [5]. In aqueous solution below a certain temperature, i.e., the transition temperature (Tt) or lower critical solubility temperature (LCST), the polymer chains remain disordered, relatively extended with a random coil conformation, and fully hydrated [12]. This hydrophobic hydration is characterized by an ordered clathrate-like water structure surrounding the apolar moieties of the polymer (Fig. 1). This structure is somewhat similar to that described for crystalline gas hydrates, although more heterogeneous and of varying perfection and stability [6, 13]. When temperature surpasses the Tt and, according to Urry's model, the polymer chains hydrophobically fold and undergo a conformational transition that leads to phase separation. That "coacervate" is composed of about of 63% water and 37% polymer [7]. In the folded state, the polymer chain adopts a dynamic, regular, non-random structure called β spiral, which involves one type II β turn per pentamer stabilized by intra-spiral inter-turn and inter-spiral hydrophobic contacts [5].
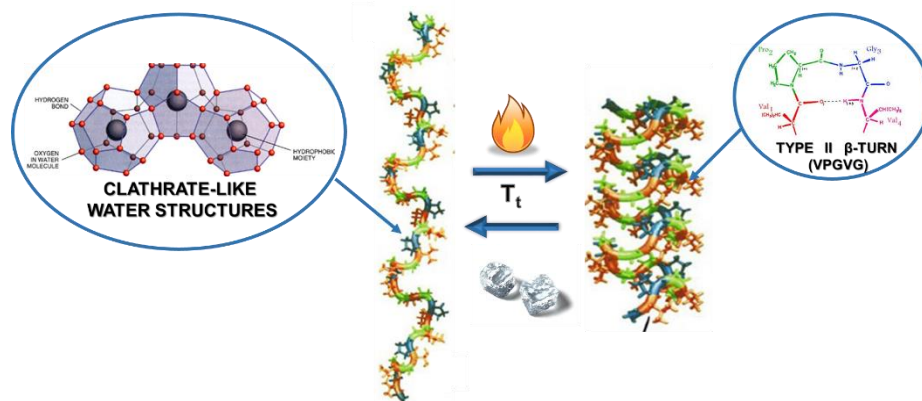
Fig. 1. Schematic representation of the thermal transition of ELRs from an extended state (low temperatures, hydrophobic moieties surrounded by clathrate water structures) to a folded state (type II β-turn in VPGVG pentapeptides).

The process begins with the formation of filaments composed of three-stranded dynamic polypeptide β-spirals, which grow up to various hundred nanometres before settling to a visible separated state [5, 8].

This process is completely reversible (lowering the temperature below Tt, the initial state is recovered) and has an associated latent heat, ΔHt [5]. This ΔHt is the result of the combination of the disruption of the water structure and the folding and stabilization owing to the Van der Waals interactions [14]. One VPGVG is enough to permit the transition from random coil to an order β turn, but higher molecular weight polymers are required to obtain materials presenting useful properties [15].

Common proteins undergo unfolding and denaturalization when temperature raises. The shift described above from a disordered state to an ordered state upon heating is the base of the inverse temperature transition (ITT). At this point, it might seems that this behavior is not possible, because it seems to violate the second law of thermodynamics. However, this apparent contradiction can be solved if the system is considered as a whole, i.e., not only the protein but also the water surrounding it. When the system moves to the ordered state, the increase in order of the protein component is less than the decrease in order of the water component. Thus, the second law of thermodynamics is indeed satisfied.

1.2.1.2   ΔT$_t$ mechanism

Previously, it has been described the capacity of mechanical work creation as a result of the temperature increment above a certain transition temperature T$_t$. It consist on a transition from a state where the molecules are extended in solution, to a phase separated state where the molecules are ordered and aggregated, consequently a mechanical work is being done. Thus, the process is a thermo-mechanical transduction.

Different methods for modification of T$_t$ have been described, most of them based on the modification of the polarity of certain functional groups present in the fourth residue of the VPGXG pentapeptide, which can exist in two different states depending on a certain external stimulus. This change in the T$_t$, as result of different hydrophobicity, open up a working temperature window in which the polymer isothermally and reversibly switches between the folded and unfolded states in response to environmental changes (Fig. 2).
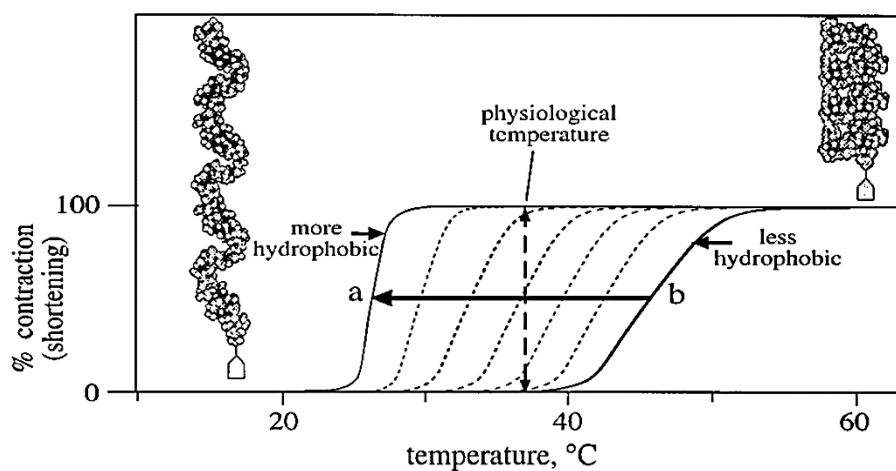
Fig. 2. Plot as a function of temperature of the contraction of ELRs of different hydrophobicities. Reproduced from [16].

This effect of changing the T$_t$ is the basis of the ΔT$_t$ mechanism and has been exploited to obtain pH, electric potential, light, chemical and other responsive interconvertible energy processes.

Experimental studies based on factors that control hydrophobic folding and assembly of ELRS resulted in a set of five phenomenological axioms for the

4

engineering of protein based materials capable of inverse temperature transitions [16]:

Axiom 1: The temperature intervals for the hydrophobic folding and assembly transition of a host protein or protein-based polymer with different guest substituents becomes a functional measure of their relative hydrophobicity.

Axiom 2: Heating to raise the temperature from below to above, the temperature interval for hydrophobic folding and assembly of macromolecules can drive contraction with the performance of mechanical work.

Axiom 3: At constant temperature, an energy input that changes the temperature interval for thermally-driven folding and assembly in a macromolecule can itself, drive hydrophobic folding and self-assembly.

Axiom 4: Two or more different functional groups of a macromolecule, each of which can be acted upon by a different energy input that changes the temperature interval for hydrophobic folding and assembly, become coupled one to another by being part of the same hydrophobic folding and self-assembling domain, that is, the energy input acting on one functional constituent alters the property of another functional constituent as an energy output.

Axiom 5: More hydrophobic domains make more efficient the energy conversions involving constituents undergoing conversion between more and less hydrophobic states.

1.2.1.3 ELRs for biomedical applications

Protein-based polymers have many advantages over conventional synthetic polymers because they are able to assemble hierarchically into stable, ordered conformations [17]. This ability depends on the structures of protein chains as well as the microenvironment. Protein-based block copolymers have the ability to form varied nanostructures in aqueous solution that provides potential benefits for biomedical applications, such as therapeutic delivery, tissue engineering, and medical imaging [18]. Similarly, they have also been applied in the field of nanotechnology due to the range of nanostructures such as nanofibres [19] or nanoparticles [20] that can be formed from them (Fig. 3).
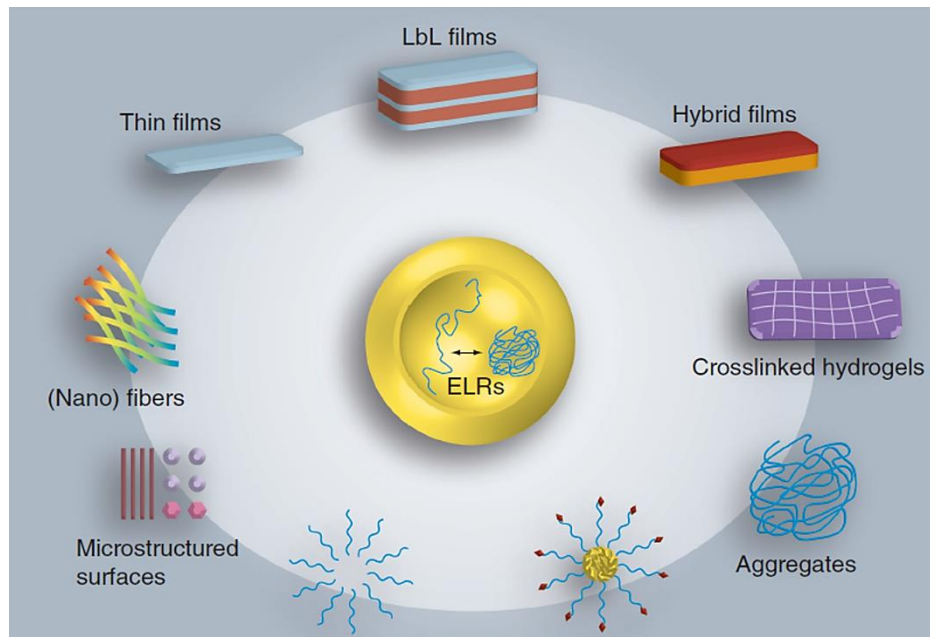
Fig. 3. Summary of the different structures that ELR-based systems can adopt for its usage in biomedical applications. Reproduced from [21].

1.2.2   Silk-like and silk-elastin-like recombinamers (SELRs)

Silk-like recombinamers (SLRs) based on the repeating motif [GAGAGS], present in the silk of the silkworm *Bombyx mori*, produce crystalline structures similar to the β-sheet structures of native silk proteins [22]. This protein is insoluble by itself, but when combined with elastin-like recombinamers (SELRs), they become soluble in cold aqueous solvents [23]. Furthermore, although ELRs are reversible when factors like temperature are modified, SELRs are irreversible because of the high hydrophobic interactions between silk motifs which conduct to crystallization [24].

By the arrangement of a repetition of the silk hexapeptide described above together with a tetrablock structure of an amphiphilic elastin-like recombinamer, a co-recombinamer is obtained, being capable of self-assembling into structures that form nanoparticles at low concentrations and hydrogels when solution collapse into a mesh at high recombinamer concentration, with a very strong stability and irreversibility.

Furthermore, there are evidences of the formation of fibres at low concentrations by SELRs [25], which increase significantly the potential applications of this material in the development of biomedical devices.

6

1.3 Enhanced Green Fluorescent Protein (EGFP)

Green Fluorescent Protein (GFP) is an auto-fluorescent protein first discovered by Shimomura et al. in 1962 in a protein extract from the jellyfish *Aequorea Victoria* [26]. This protein is able to emit intense and stable fluorescence without the presence of any cofactors and in a very wide range of conditions (pH, temperature, salts) [27-29], which makes it very useful for molecular biology applications such as markers for gene expression analysis, tracking of analytes within cells or organelles [28, 30]. Other nanotechnological approaches can also take advantage of GFP by the inclusion of this protein in delivery systems or biomedical devices to allow tracking of materials through an organism [31-33]. Crystal structure of GFP can be observed in Fig. 4 [34].
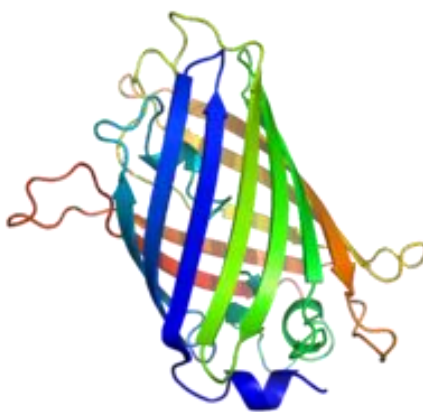
Fig. 4. Green Fluorescent Protein crystal structure.

As the intrinsic fluorescence of wild type GFP (wtGFP) remains on an excitation peak at 395nm, which is out of the range of a fluorescence-activated cell sorting instrument, and leads to an emission peak at 509nm that has medium intensity, some mutants in different residues of GFP were studied in order to overcome these drawbacks. Hence, a mutant F64L and S65T was reported as the best candidate [35], having an excitation wavelength of 488nm and various emission ones, being one of them at 530nm, having a higher fluorescence intensity than wtGFP (35-fold increase).

Therefore, EGFP was chosen for the fusion to an SELR in order to achieve a great fluorescence intensity and excitation at 488nm which is useful for further applications in visualization and sorting techniques.

2. MATERIALS AND METHODS

2.1. Materials

2.1.1. Chemical reagents

All the reagents employed on this work are listed on Table 1.

Reactive	Brand
Acrylamide/Bis-acrylamide	Amresco
AEBSF	Apollo Scientific
Agarose Seakem.	Cambrex
Ammonium persulphate (APS).	Sigma-Aldrich
Ampicillin	Apollo Scientific
Bromophenol blue	Sigma-Aldrich
Chloridric acid	Merck
Copper chloride	Sigma-Aldrich
Dimethyl sulfoxide (DMSO)	Carlo Erba
E-64	Apollo Scientific
Ethanol	Merck
Ethylenediaminetetraacetic acid (EDTA)	Sigma-Aldrich
Glycerol	Sigma-Aldrich
Glycine	Sigma-Aldrich
Leupeptin	Apollo Scientific
Pepstatin A	Apollo Scientific
Phenylmethylsulfonyl fluoride (PMSF).	Apollo Scientific
Phosphate buffered saline (PBS)	Gibco
Sodium chloride (NaCl)-	Sigma-Aldrich
Sodium dodecyl sulfate (SDS)	Sigma-Aldrich
Sodium hydroxide	Sigma-Aldrich
Tetramethylethylenediamine (TEMED).	Sigma-Aldrich
Ultrapure water	Millipore
β-Mercaptoethanol.	Sigma-Aldrich

Table 1. Reagents list

2.1.2   Other materials

Glass material was conveniently washed with detergents if needed and rinsed with distilled wáter prior use.

Other materials, such us tips, microtubes, falcon tubes, etc. are bought sterile or are sterilized on an autoclave (Autotester E-75) for 20 minutes at 121ºC and 1 atm pressure.

2.1.3   Molecular biology materials

2.1.3.1   Restriction enzymes

The restriction enzymes used in this work are listed below:

DpnI, EcoRI, SapI, Eam1104I (Thermo Fisher).

All enzymes are used according to the manufacturer instructions.

2.1.3.2   Other enzymes

During the realization of this work the following enzymes have been employed, being all of them purchased to Thermo Fisher and used under the suggested conditions: *T4 DNA Ligase, Shrimp alkaline phosphatase (SAP), FastAP Phosphatase* (Thermo Fisher).

2.1.3.3   Cloning and expression vectors

The DNA fragments employed were cloned in pDrive cloning vector (Qiagen), exposed in Fig. 5 by genetic engineering methods using the enzymes listed above following manufacturer instructions.

Fig. 5. pDrive cloning vector.

For the expression of the different recombinant polymers a p7 expression vector has been employed (Fig. 6). The p7 plasmid was constructed in our laboratory from Novagen's pET-25b (+) vector, by Dr. A. Girotti.

Fig. 6. Scheme of p7 plasmid based on Novagen's pET-25b(+) vector.

10

2.1.3.4   Other reagents

Three kits were used for the plasmid and DNA purification either from an *Escherichia coli (E.coli)* culture or from an agarose gel: *NucleoSpin Plasmid* (Macherey-Nagel), *Quantum Prep Plasmid Midiprep Kit* (Bio-Rad) and *PureLink Quick Gel Extraction Kit* (Life Technologies).

2.1.4   Bacterial strain

During the realization of this work different strains of *E.coli* for plasmid transformation have been employed: *XL1-Blue Subcloning Grade* and *XL1-Blue Competent Grade* (Stratagene).for plasmid cloning and *BL21(DE3) Star* (Invitrogen) and *BLR(DE3)* (Novagen) for plasmid expression.

2.1.5   Culture media

The culture media used for bacterial growth and transformation are listed below:

- *Luria-Broth (LB)* (Pronadisa): Concentration 25 g/L.
- *Terrific Broth (TB)* (Formedium): 55.85 g/L supplemented with 8 mL/L Glycerol (Fisher).
- *LB-Agar:* LB 25 g/L + 1.5% (w/v). Agar (Fluka).
- *SOC Broth* (Sigma Aldrich).

2.1.6   Buffers

The buffers employed along this work are the following:

- *PBS*: 5 mM Na_2HPO_4 (pH 7.4), NaCl 140 mM.
- *TAE:* 40 mM Tris-acetate (pH 8), 1 mM EDTA.
- *TBS (washing buffer)* :20 mM Tris-base (pH 8), 140 mM NaCl.
- *TE (sonication buffer):* 10 mM Tris-base (pH 8), 1 mM EDTA, 1mM PMSF.
- *Running buffer for SDS-PAGE:* Tris-base 25 mM (pH 8.3), Glycine 192 mM, SDS 0,1% (w/v).

- *DNA loading buffer for agarose gel electrophoresis:* 30% (v/v) glycerol, 0.1% (w/v) SDS, 0.05% (w/v) bromophenol blue (BPB), 50mM Tris-base (pH 8), 0.05 mM EDTA.

- *Protein loading buffer:* Tris-base 1M (pH 6.5), 312.5 mM, SDS 10% (w/v), Glycerol (v/v), β-Mercaptoethanol 25% (v/v), bromophenol blue (BPB) 2% (v/v).

All the solutions were prepared using ultrapure water (Millipore).

2.1.7   Elastin-like recombinamers (ELRs)

All the elastin-like recombinamers (ELRs) employed in the development of this work have been designed and produced in our laboratory (G.I.R. Bioforge) by recombinant DNA techniques. DNA corresponding the amphiphilic backbone plus a silk domain, named $(EIS)_2$, was constructed by A. Fernández-Colino, while EGFP gene was first cloned into a pDrive vector by M. Pierna. For the purpose of this work, $(E_{50}I_{60}Silk)_2$-EGFP (also named $(EIS)_2$-EGFP or SELR-EGFP) was specifically designed and produced while HRGD6, a recombinamer used for a layer by layer approach, with a 6 times repetition of a cell adhesion bioactive sequence was already part of Bioforge's list of recombinamers.

The production was done in *E.coli* fermentation (see Methods) and purified taking advantage of both the smart nature and the reversible thermo-dependent segregation showed by this kind of materials, by inverse transition cycling (ITC).

The abbreviation, molecular weight (Mw), and amino acid sequence of both SELR-EGFP and HRGD6 recombinamers are shown in Table 2.

Elastin-like recombinamer (SELR) abbreviation	Amino acid sequence	Molecular weight (Mw)
HRGD6	MGSSHHHHHHHHGLVPRGSHMESLLP-$[1]_6$-V	60600 Da
(EIS)$_2$-EGFP or SELR-EGFP	MESLLP-[[(VPGVG)$_2$-VPGEG-(VPGVG)$_2$]$_{10}$-(VGIPG)$_{60}$-[V(GAGAGS)$_5$]$_2$-G]$_2$-VMASKGEELFTGVVPILVELDGDVNGH-KFSVSGEGEGDATYGKLTLKFICTT-GKLPVPWPTLVTTLTYGVQCFSRYPD-HMKQHDFFKSAMPEGYIQERTIFFE-DDGNYKSRAEVKFEGDTLVNRIELTGT-DFKEDGNILGNKMEYNYNAHNVYIM-TDKAKNGIKVNFKIRHNIEDGSVQLADH-YQQNTPIGDGPVLLPDNHYLSTQS-ALSKDPNEKRDHMILLEFVTA-AGITHGMDELYKV	127622 Da

Table 2. Amino acid composition and molecular weight of the elastin-like recombinamers used in this work.

2.2   Methods

2.2.1   *DNA agarose gel electrophoresis*

DNA agarose gel electrophoresis is a technique used to separate and check the appearance and size of DNA of the fragments obtained from an enzymatic digestion with the endonucleases listed above. Different concentrations (in 1x TAE), are applied according the sizes of the DNA fragments and the kind of gel, analytical or preparative, being the first one the used to assess the rightness of a purified plasmid and the latter to obtain DNA fragments for further use. In Table 3 different agarose concentrations and their resolution capability are listed.

Fragment size (bp)	Agarose final concentration % (w/v)
800-10000	0.8
400-8000	1
300-7000	1.2
200-4000	1.5
100-2000	2

Table 3. Resolution in electrophoresis of different agarose gel concentrations.

The gels are prepared in a glass-made Erlenmeyer flask by adding the quantity of agarose and volume of TAE 1x required for each concentration. The agarose is melted in a microwave. Once melted the flask is weighted and ultrapure water (MQ) is added until reaching the initial weight, thus maintaining the initial concentration and gel uniformity. After cooling down to 60°C, the gel is casted in a horizontal tray with the desired comb.

DNA loading buffer 5x is added to the samples to reach a 1x concentration. A fixed voltage, between 2 and 7 V/cm – according to each sample, is then applied. The electrophoresis is run having as references the colored markers (Table 4). Last, the gel is stained for 10 to 30 minutes in a 1x Gselred solution, and the DNA bands are visualized by exposition to UV light in a Viber Lourmat, TFX-20M transilluminator.

TAE 1x –BPB	Agarose concentration % (w/v)
2900	0.3
1650	0.5
1000	0.75
500	1
370	1.25
200	1.75
150	2

Table 4. Relation between linear DNA migration and bromophenol blue (BPB)

2.2.2 *Plasmid purification*

The plasmids employed in this work were purified using the commercial kits listed above following the manufacturer's instructions. DNA was eluted with Elution Buffer from the kit or ultrapure water. For applications were higher DNA concentration is required only half of the recommended elution volume is used and the elution buffer is used at 65°C to enhance the purification yield.

2.2.3 *DNA digestion with restriction enzymes*

Reaction conditions (temperature, concentration, time of reaction, buffer) for the digestion are supplied by the enzyme manufacturer. The rate of digestion is controlled by DNA agarose gel electrophoresis.

2.2.4 *DNA dephosphorylation*

Dephosphorylation reaction conditions (temperature, time of reaction, buffer) are supplied by the phosphatase manufacturer. For the p7 expression vector two different consecutive phosphatases were used and the incubation time was enlarged until one hour to assure the correct dephosphorylation.

2.2.5 *DNA fragments purification from an agarose gel*

The target DNA band is first separated by electrophoresis and visualized in an agarose gel of an appropriated concentration and stained with RedGel. Secondly, the band is extracted from the gel with the help of a scalpel. Minimum quantity of agarose should be cut during band extraction.

The purification of the fragment is carried out using the commercial kit *PureLink Quick Gel Extraction Kit* (Life Technologies) following the protocol indicated by the manufacturer.

2.2.6 *Ligation reaction*

The reaction ligation is carried out at a final volume of 10-12 µL by mixing the insert with the vector, in a molar relation from 1:1 to 5:1, and T4 DNA ligase as enzyme with its corresponding buffer following the specifications indicated by the supplier. The reaction is conducted during 1 hour at room temperature. The ligation

reaction is interrupted by the inactivation of the T4 DNA ligase by incubation during 10 minutes at 70°C.

2.2.7   *Cloning on the pDrive/p7 vector*

Once the ligation reaction is concluded, a certain quantity of the ligation solution is used to transform competent cell as specified below.

2.2.8   *Transformation of competent cells*

2.2.8.1   *Transformation of XL1 blue subcloning grade competent cells*

This bacterial strain has an efficiency $\geq 10^6$ transformants per microgram of DNA. Plasmid DNA to be amplified by cloning is transformed in this bacterial strain following the protocol specified by the supplier.

2.2.8.2   *Transformation of XL1 blue competent cells*

This bacterial strain has an efficiency $\geq 10^8$ transformants per microgram of DNA. Ligation products were transformed into this bacterial strain following the protocol specified by the supplier.

2.2.8.3   *Transformation of BLR(DE3) competent cells*

This bacterial strain is transformed with the expression plasmid p7 following the chemical method TSS reagent ("Transformation and Storage Solution") [36].

A single colony, isolated and grown in a LB-agar plate, is used to inoculate 10 mL of LB medium and grown at 37ºC with shaking (250rpm), until reach a OD_{600}=0.3-0.4. At this point, the metabolism and cell growth is stopped by incubation on ice for 5 minutes. The cell suspension is centrifuged at 3000rpm (1100xg) for 10 minutes at 4ºC. The supernatant is discarded and the pellet is re-suspended in 1 mL of cold TSS x1 solution. About 1-10 ng of plasmid in final volume of 1-10µL (at least 2µL) are added to the mix. The cellular suspension plus the plasmid DNA are kept on ice for 30 minutes followed by a heat shock at 42ºC in a water bath for 2 minutes. The heat shock is stopped by immersion on ice for additional 2 minutes. 1mL of warm LB is added and the suspension is incubated one hour at 37ºC with shaking (250rpm). Finally, 200-500µL of the transformation mix is plated in LB-agar plus the antibiotic plates that are incubated for 16-20 hours at 37ºC (see Fig. 7).
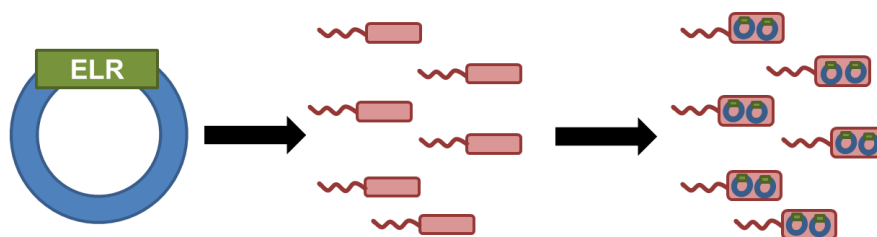
Fig. 7. Schematic representation of ELR transformation process to a BLR(DE3) expression _E.coli_ strain.

2.2.9   Glycerol stock preparation

Positive clones of expression strains like BLR(DE3), which are of special interest, selected by SDS-PAGE electrophoresis, are grown at 37°C with shaking (250rpm) on LB with 0.5% of glucose (for the expression strains) and antibiotic at the optimal concentration, until reaching an OD_{600}=0.6-0.8. Then, 0.1 volumes of 80% (v/v) sterile glycerol and 0.9 volumes of cell suspension are added to a cryovial and stored at -80ºC.

2.2.10   Production and purification of recombinant polymers

2.2.10.1 Production of ELRs

During the biosynthesis of SELR-EGFP, the expression vector p7 has been employed. p7 has been obtained in our laboratory by mutagenesis of pET25b (+) by Dr. Alessandra Girotti. The final constructions were transformed on the bacterial strain BLR(DE3) following the above mentioned protocol.

SELRs expression starts inoculating the desired colony in liquid LB medium plus antibiotic at 37°C with orbital shaking (250rpm) during approximately 6 hours. This culture is used as inoculum for a fresh TB medium (plus antibiotic), in a volume ratio of 1:500.

For large batches production, as this case, a 15L Bioreactor is used (Applikon Biotechnology), allowing the full control of variables like temperature, pH, OD_{600} and oxygen concentration, regulating all of them if needed, improving the yield of the bioproduction process. It is inoculated with 1L of the pre-incubated cell suspension to a final volume of 15L of TB medium and fermentation time varies

from 14 to 16h, setting temperature at 37ºC, pH at 7, oxygen control at 50% of the initial oxygen concentration and stirring at 499rpm.

2.2.10.2 Bacteria disruption

Once the induction is finished, the bacteria's metabolism and growth are stopped by cooling it down to 4ºC and cells are centrifuged and washed with washing buffer until having a clear supernatant. Then, the cell pellet is re-suspended in 25 mL of TE per liter of culture. Cell suspension is kept at 4ºC and protease inhibitors (PMSF, AEBSF, E-64, Pepstatin A, Leupeptin) are added to the desired concentration to avoid ELR degradation by *E.coli* proteases.

Bacteria are disrupted (lysated) by changing pressure disruption employing a Constant Cell Disruption System (Model TS 0.75KW, Constant System). Finally, the lysate is centrifuged at 4ºC for 60 minutes at 15000xg. The supernatant contains the recombinant polymer biosynthesized.

2.2.10.3 Purification of ELR

The purification of ELRs starts from the supernatant obtained at the end of the lysis process, taking advantage of the ELRs' smart nature and inverse temperature transition (ITT). Therefore, the purification process is based on successive cycles of precipitation (heating) and resuspension (cooling) of the supernatant, named Inverse Transition Cycling (ITC). In order to reduce the Transition temperature (Tt) and facilitate the precipitation of the ELRs, NaCl is added during the purification process until a 1M concentration is achieved.

Finally, after the last purification cycle, the re-suspended polymer is dialyzed against cold ultrapure water. The solution is then adjusted to pH 7, frozen, lyophilized and stored at -20°C. Purification steps, as well as the final product, are checked by polyacrylamide gel electrophoresis.

2.2.11 Denaturing polyacrylamide gel electrophoresis

The protein polyacrylamide gel electrophoresis in the presence of sodium dodecyl sulfate –SDS-PAGE– is made following the protocol for discontinuous

systems described by Laemmli [37] to achieve the separation of a mixture of proteins in a sample, being the gel composed of two different sub-gels: stacking and resolving.

The proteins' effective charge almost does not differ because the SDS strongly interacts with proteins providing them with approximately one negative charge per each amino acid residue The SDS completely denatures the proteins by breaking the non-covalent interactions responsible for the quaternary and tertiary structure. Besides, a reducing agent (β-mercaptoethanol) is added to the samples in the protein loading buffer in order to break the disulfide bonds that might exist. The reducing and denaturing process is facilitated with the heating of the samples during 5 minutes at 95ºC.

A "MiniVE vertical electrophoresis system" from Hoefer (Amersham Pharmacia Biotech, Pittsburg, USA) electrophoretic system was employed to perform the polyacrylamide electrophoresis. The total percentage of acrylamide (%T) in the resolving gel varies according to the molecular weight of the polypeptide we want to separate. A 10%T resolving gel was used in every SDS-PAGE experiment with the following composition (Table 5):

Reactive	Resolving gel	Stacking gel
Acrylamide 40%	10% (w/v)	4% (w/v)
Tris-HCl pH 8.8	375 mM	-------
Tris-HCl pH 6.8	-------	125 mM
SDS 10%	0.1% (w/v)	0.1% (w/v)
APS 10 %	0.05% (w/v)	0.05% (w/v)
TEMED	0.05% (w/v)	0.08% (w/v)

Table 5. Gel composition for SDS-PAGE.

A molecular weight marker (Unstained Protein Molecular Weight Marker, Thermo Fisher) is loaded together with the samples in order to know the molecular weight of each band.

Staining is performed according to Lee's method [38]: 10 minutes incubation at room temperature of the gel in a 0.3M Copper chloride solution followed by a washing step in distilled water for 5 minutes. Pictures are taken by *Gel Logic 100 Imaging System* camera system and *Kodak 1D Image Analysis* (Kodak) software.

2.2.12   Nanoparticle formation

2.2.12.1 $(EIS)_2$-EGFP nanoparticles

SELR-EGFP nanoparticles were formed by the dissolution of lyophilized recombinamer in ultrapure cold water or cold PBS at different concentrations: 10, 5 and 2 mg/mL. Samples were filtered with a 0.45µm filter to eliminate dust particles and then, each concentration of the samples dissolved in water was aliquoted in different tubes for following adjusting to different pH (4, 7 and 10.5). Tubes were stored at 4ºC until use in DLS experiments or in a plate reader for the measurement of the fluorescence intensity (see 2.2.15.1 and 2.2.15.5).

2.2.12.2 Layer by Layer nanoparticles

For the purpose of obtaining $(EIS)_2$-EGFP nanoparticles covered with HRGD6 by charge interactions between COO^- groups of glutamic acid residues in the first one and NH_3^+ groups of lysine residues in the latter, SELR-EGFP solutions were prepared by the dissolution of lyophilized recombinamer at different concentrations in ultrapure water: 1, 0.5 and 0.2 mg/mL. Samples were filtered with a 0.45µm filter to eliminate dust particles. This lower concentrations than the ones prepared for DLS experiments are due to the possibility of particle aggregation when HRGD6 is added to the suspension if higher concentrations are used.

Solutions were placed in a water bath at 37ºC on a magnetic stirrer (MR Hei-Tee, Heidolph) and a specified volume (depending on the charges ratio) of a 10 mg/mL HRGD6 solution (ultrapure water) was added drop by drop to the SELR-EGFP suspension with strong stirring and mixture was left at this conditions for 30 minutes for further stabilization. $NH_3^+:COO^-$ ratios used were 1:1, 2:1 and 5:1 for initial z-potential measurements and 5:1 and 10:1 for final cell culture experiments.

2.2.13   Cell culture experiments

Cell culture experiments were performed with HFF-1 (human fibroblasts) cell line (ATCC, SCRC-1041). Medium used was DMEM GlutaMAX (Life Technologies) without the addition of serum to avoid particle adhesion to serum proteins.

First, cells were seeded on a 48-well plate, at a concentration of 10000 cells/well in a volume of 200μL of medium and it was incubated overnight at 37ºC, 5% CO_2 (Steri-Cycle CO_2 Incubator, Thermo Fisher). Afterwards, 5 mL of DMEM were supplemented with 500μL of micro and nanoparticle suspension obtained by LbL, either of 1 or 0.5 mg/mL concentration to test both conditions. Then, medium in the wells was replaced by the supplemented one (200μL per well) and incubated at 37ºC and 5% CO_2 for 2 hours and then for 24 hours.

Photographs were taken with a Nikon ECLIPSE Ti microscope coupled to a Digital Sights DS-2MBWc camera with the software NIS Elements (Nikon).

2.2.14   Hydrogel formation

Hydrogels were formed dissolving SELR-EGFP either in ultrapure water or PBS at a concentration of 125 mg/mL in an eppendorf tube during 16h at 4ºC in a rotational shaker. After complete dissolution, incubation at 37ºC was performed during 24h, taking pictures of the gel at 1h, 2h, 4h and 24h excited with visible and UV light to monitor the hydrogel formation.

2.2.15   Experimental techniques

2.2.15.1 Dynamic light scattering

Dynamic light scattering (DLS) is a technique for measuring the size of particles normally in the sub-micron region. Typically, DLS is concerned with measurements of dispersed particles or suspended macromolecules in a liquid medium, measuring the particles Brownian motion and relating it to the particles' size.

Brownian motion is the random movement of particles suspended in a fluid due to their collision with the solvent molecules that surround them. Thus, the random motion will be affected by different factors, mainly the size of the molecules (the bigger the molecules, the slower they move), the viscosity of the solvent (the more viscous the solvent, the slower the molecules move) and temperature. Temperature is a crucial parameter, both temperature stability and temperature accurate knowledge are required, due to its influence on the solvent viscosity and owing to, temperature instability will lead to convection currents in the sample, thus non-random motion, resulting in incorrect size interpretation.

The velocity of the Brownian motion is defined by the translational diffusion coefficient (D), which is used to calculate the size of the particles by using the Stokes-Einstein equation:

$$D_h = \frac{k_B T}{3\pi\eta D}$$

Where k_B is the Boltzmann constant, T is the temperature and η is the viscosity. It is worth noting, that DLS refers to how a particle diffuse within a fluid so the calculated diameter is a hydrodynamic diameter (D_h), (effective molecule diameter plus hydration layer).

Light scattering measurements were performed using a Zetasizer nano ZSP (Malvern instruments) equipped with a 10mW He-Ne laser at a wavelength of 633nm. Size data were obtained at 37ºC (above Tt).

2.2.15.2 Zeta potential

ζ-potential analysis is a technique for determining the surface charge of nanoparticles in solution. The ζ-potential of the ELR and Layer by Layer (LbL) obtained nanoparticles was monitored at 37ºC (above Tt) using a Zetasizer nano ZSP apparatus (Malvern instruments). Measurements were carried out in a range of SELR-EGFP concentrations and HRGD6:SELR-EGFP (or more precisely, NH_3^+:COO^-) rates. The ζ-potential values, which were determined using the Smolukowski equation relating ionic mobility to surface charge, were plotted as the average of 10 repeated measurements.

2.2.15.3 Differential scanning calorimetry (DSC)

Differential scanning calorimetry (DSC) is a technique in which the difference in the amount of heat required to increase the temperature of a sample and reference is measured as a function of temperature.

DSC experiments were performed using a Mettler Toledo 822e with a liquid-nitrogen cooler. The solutions were prepared at 50 mg/mL either in ultrapure water (MQ) at different pH, above and below the pKa of COOH side chain groups, or in PBS. For analysis, 20µL of the solution was placed in a standard 40µL aluminum pan and sealed hermetically. The same volume of MQ or PBS was placed in the reference pan.

2.2.15.4 Fourier Transform Infrared Spectroscopy

FTIR analysis was conducted with a BRUKER TENSOR 27 spectrometer. A 64 scan spectrum was collected at single beam absorption mode with a 4 cm^{-1} resolution in an interval from 4000 to 600 cm^{-1}. Calculations were done by OPUS software (Mattson Instrument Inc.).

2.2.15.5 Measurement of fluorescence intensity

Fluorescence intensity was measured at every condition by the addition of 100uL of each sample to a 96-well plate and the introduction into a plate reader (SpectraMax M2e, Molecular Devices), setting λ_{ex} = 488nm and λ_{em} = 530nm.

2.2.16   Experimental techniques performed by external services

2.2.16.1 Amino-acid analysis

The amino acid composition of the ELR employed during this work was determined by *Laboratorio de Técnicas Instrumentales (LTI, University of Valladolid)*.

After addition of a known quantity of α-aminobutyric acid as internal pattern the samples were hydrolyzed (6M HCl, 1% Phenol and 2.5 hours of incubation at 155°C) and evaporated. The powder was resuspended in 1mL of 20mM HCl and a 1/10 dissolution was prepared. The quantification of the less represented amino acids was made from the most concentrated sample and the quantification of the most

represented amino acids from the 1/10 dissolution. One aliquot of each dissolution was derivatized according to the AccQ-Tag Waters method and analyzed by HPLC with UV detection, using a WATERS600 HPLC gradient system with a WATERS2487 detector.

2.2.16.2 MALDI-TOF

Determination of the SELR-EGFP molecular weight was made by MALDI-TOF at the *Laboratorio de Técnicas Instrumentales (LTI, University of Valladolid).*

2.2.16.3 Transmission electron microscopy (TEM)

TEM measurements were conducted using a JEOL JEM-1230 electron microscope (cicBiogune, Bilbao) operating at 120 kV, in order to visualize the structures formed by $(EIS)_2$-EGFP recombinamer. Specimens were prepared by placing a drop of a 2 days 37ºC incubated stabilized solution (10 mg/mL in PBS) at the corresponding temperature on a preheated plasma-treated carbon-coated copper grid, followed by water evaporation at the same temperature. Samples were stained with uranyl acetate solution (1.0 wt %) to enhance the contrast of the nanoparticles.

3 RESULTS AND DISCUSSION

3.1 Design, construction and recombinant production of $(E_{50}I_{60}Silk)_2$-EGFP

The combination of previous and recent work in our group, the first ones regarding the construction of amphiphilic ELRs, that showed a thermoresponsive gel formation at high concentrations [39], and the others concerning the addition of a silk domain in order to add strength to the hydrophobic interactions that stabilize the structure [23, 24], led us to the design of a naturally fluorescent hydrogel based on SELRs, by the fusion of the Enhanced Green Fluorescent Protein to the SELR backbone capable of forming very stable hydrogels (Fig. 8).
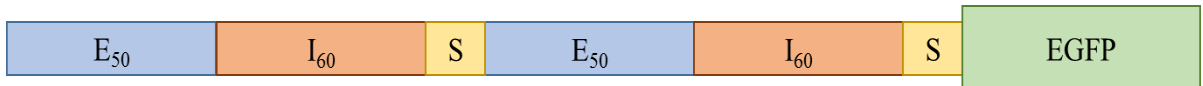

| E_{50} | I_{60} | S | E_{50} | I_{60} | S | EGFP |

Fig. 8. SELR-EGFP schematic representation. E_{50} stands for $[(VPGVG)_2\text{-}VPGEG\text{-}(VPGVG)_2]_{10}$; I60 for $(VGIPG)60$; S for silk motif repetitions and EGFP for Enhanced Green Fluorescent Protein sequence.

The construction of $(E_{50}I_{60}Silk)_2$-EGFP gene was performed following the guidelines described in materials and methods . The gene construction was assessed by agarose gel electrophoresis in every step of the process, as showed in Fig. 9.
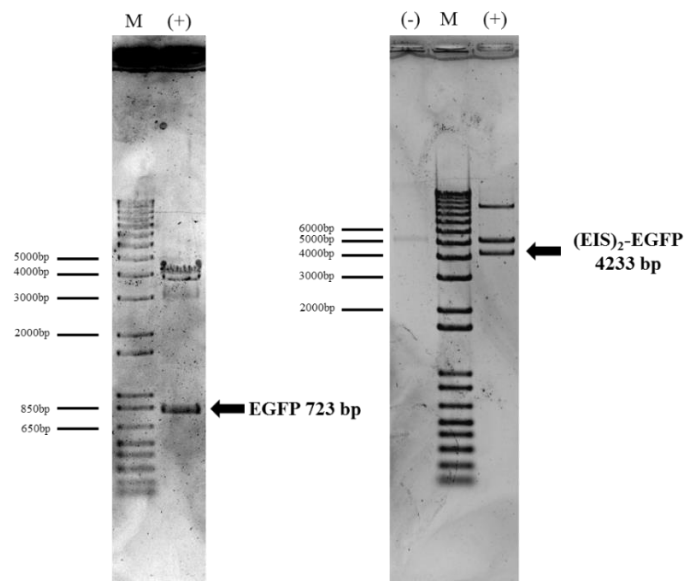

Fig. 9. Agarose gel electrophoresis of two different steps in the SELR-EGFP gene construction procedure.

Finally, gene construction was achieved and subsequent production was done, by the transformation of a protein expression bacterial strain named BLR(DE3). Expression was qualitatively assessed by SDS-PAGE (Fig. 10) and quantitatively by the measure of fluorescence in a bacterial suspension (Fig. 11). Colonies were selected for their high expression, combining both qualitative and quantitative results. Negative control (NC or (-)) was a non-expressing colony for both experiments.
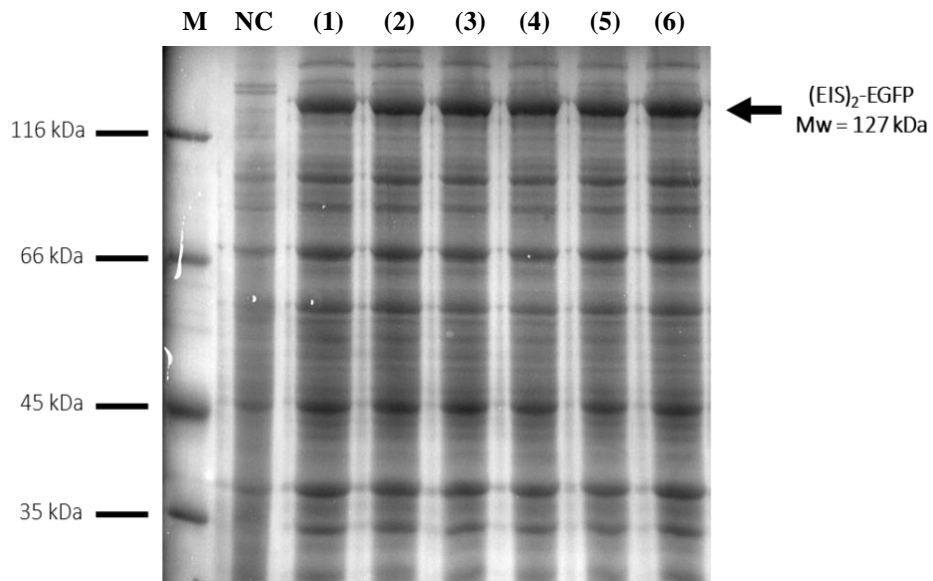

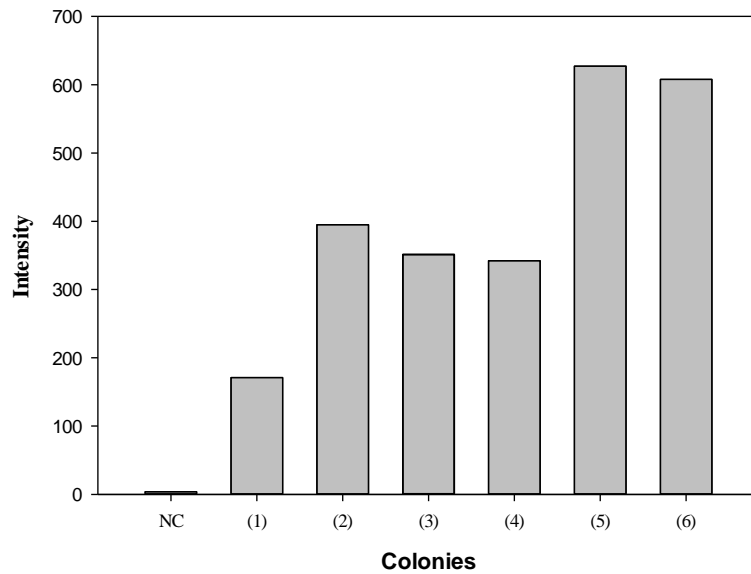**Fig. 10. SDS-PAGE of *E.coli* colonies expressing SELR-EGFP.**

Fig. 11. Fluorescence intensity of the studied colonies.

26

By means of these results, colonies (5) and (6) were selected for the subsequent scaled-up expression and production.

Bacteria could also be observed in a fluorescence microscope (Fig. 12), although a high green background can also be seen, small points corresponding bacteria can be detected.
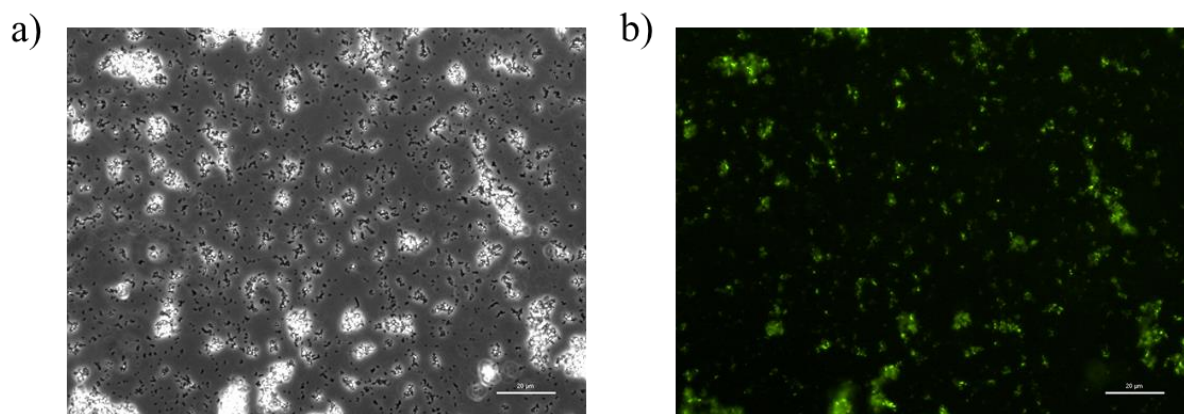

Fig. 12. SELR-EGFP expressing bacteria observed by a) phase contrast and b) fluorescence microscopy.

The purification procedure described in materials and methods was improved by the repetition of the production and purification processes giving as a result a pure fluorescent recombinamer, which could be observed by SDS-PAGE (Fig. 13). Lanes loaded with samples where SELR-EGFP is dissolved are pointed out with a + symbol, while a − refers to sample without SELR-EGFP, although some fraction of the recombinamer can be found where not supposed to, due to lack of total recovery in the resuspension step.
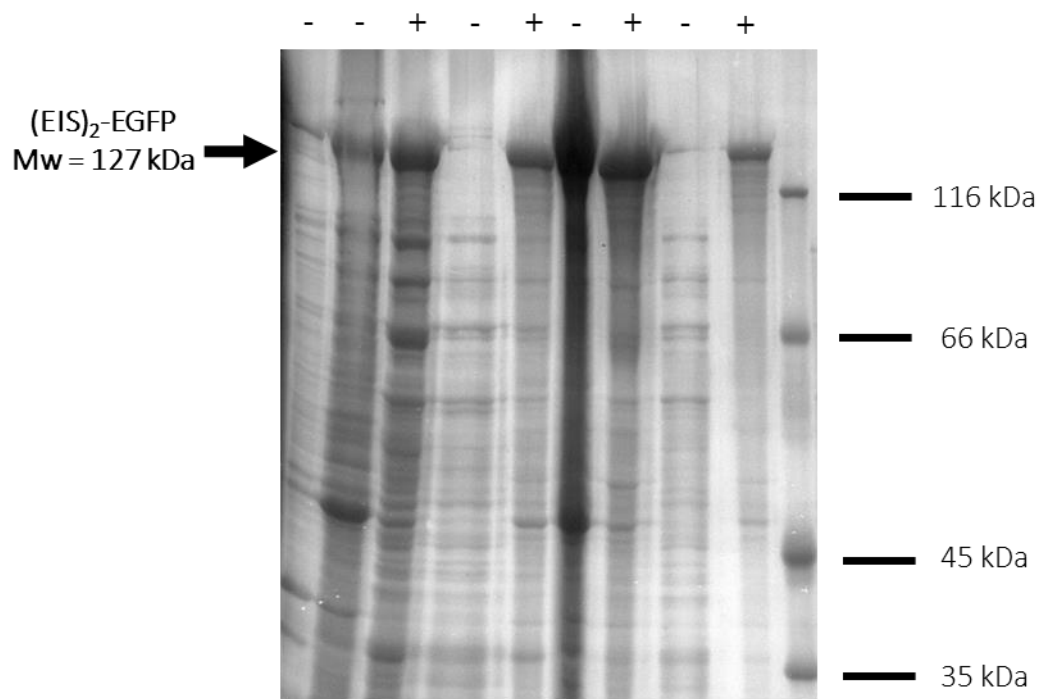
Fig. 13. SDS-PAGE of ITC steps during SELR-EGFP purification.

In every step of the inverse transition cycles (ITC) conducted to get pure SELR-EGFP, fluorescence could be observed when the solution as well as the pelleted SELR was exposed to an excitation source (UV lamp), as can be seen in Fig. 14. Some contaminants could be seen in the first ITC steps, while the pure SELR solution was perfectly green, not only fluorescent but also when excited to visible light, concluding that fusion of EGFP to an SELR is a very useful approach for simple and rapid purification of EGFP, without the need of further downstream process like chromatography or other purification techniques.
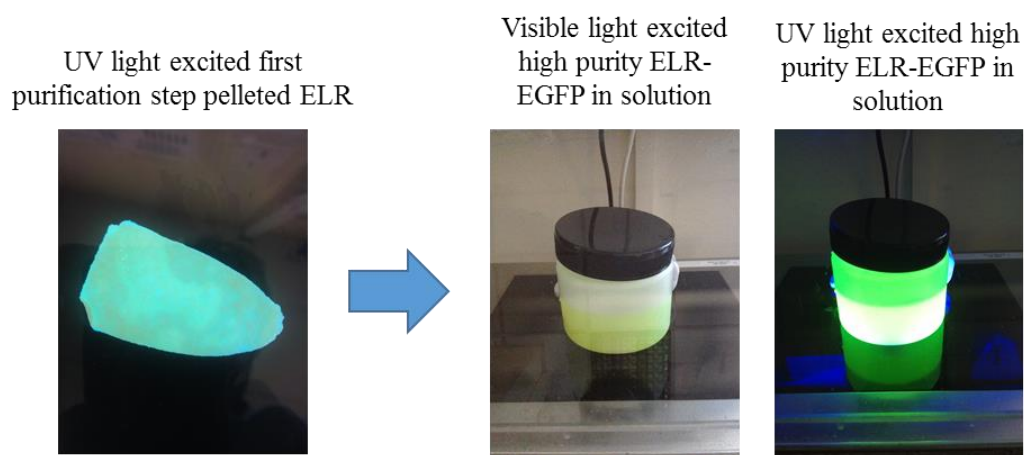
UV light excited first
purification step pelleted ELR

Visible light excited
high purity ELR-
EGFP in solution

UV light excited high
purity ELR-EGFP in
solution

Fig. 14. SELR-EGFP fluorescence during ITC purification procedure.

3.2 (E$_{50}$I$_{60}$Silk)$_2$-EGFP physicochemical characterization

Characterization was carried out by the preparation of a lyophilized sample, accordingly to the requirements of each technique.

3.2.1 Evaluation of lyophilized SELR-EGFP pureness and molecular weight by SDS-PAGE

SDS-Polyacrilamide Gel Electrophoresis of the ultra-pure water solubilized freeze-dried recombinamer confirm the 99% purity of the final (EIS)$_2$-EGFP recombinant protein, although residual degradation can be observed (Fig. 15), not having any influence in the fluorescence of the material.
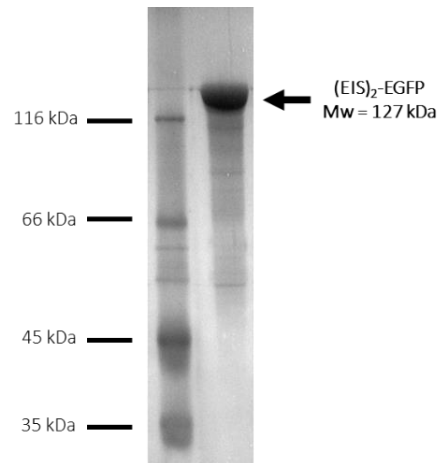
Fig. 15. SDS-PAGE of lyophilized SELR-EGFP at a concentration of 1 mg/mL.

3.2.2 Determination of SELR-EGFP molecular weight by MALDI-TOF mass spectrometry

MALDI-TOF mass spectroscopy result was not totally satisfactory, as the peak corresponding to the whole $(E_{50}I_{60}Silk)_2$-EGFP, with a molecular weight of 127 kDa, did not appear. However, the peaks corresponding to the di and tri-ionized SELR molecules are present, suggesting the existence of the complete protein (Fig. 16).

Another peak can also be seen, which corresponds to a degradation peak. It is important to take into account that this technique is not quantitative, and must be compared with the data extracted from SDS-PAGE. By means of this comparison, it can be observed that the degraded SELR is a very minor fraction of the whole sample.
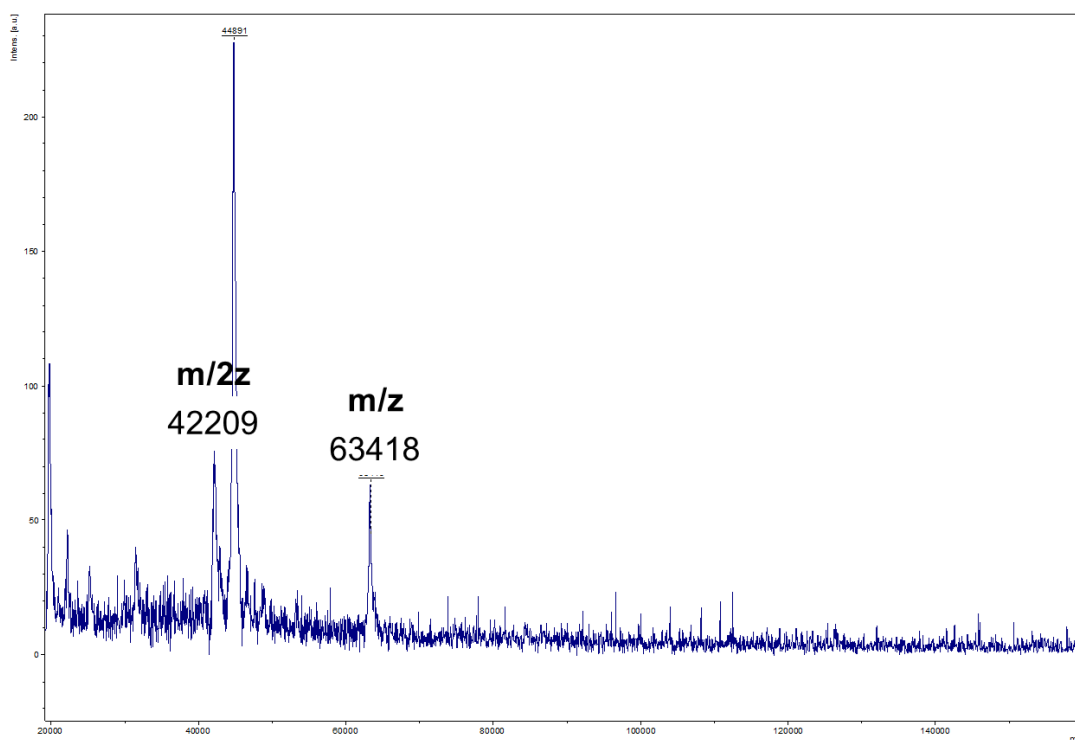
Fig. 16. MALDI-TOF mass spectrometry spectrum of SELR-EGFP.

3.2.3 *Secondary structure analysis of SELR-EGFP by Fourier Transform Infrared (FTIR) spectroscopy*

Fig. 17 corresponds to the Fourier Transformed Infrared spectrum of $(EIS)_2$-EGFP. Peaks near 1650 cm^{-1} refer to amide I band, as a result from the C=O stretching vibrations of the peptide bond, while peaks near 1540 cm^{-1} and 1240 cm^{-1} are named amide II and amide III bands, respectively. The peak near 3300 cm^{-1} is thought to be due to N-H stretching vibrations and the peak near 1400 cm^{-1} to result from protein side chain COO^- [40].
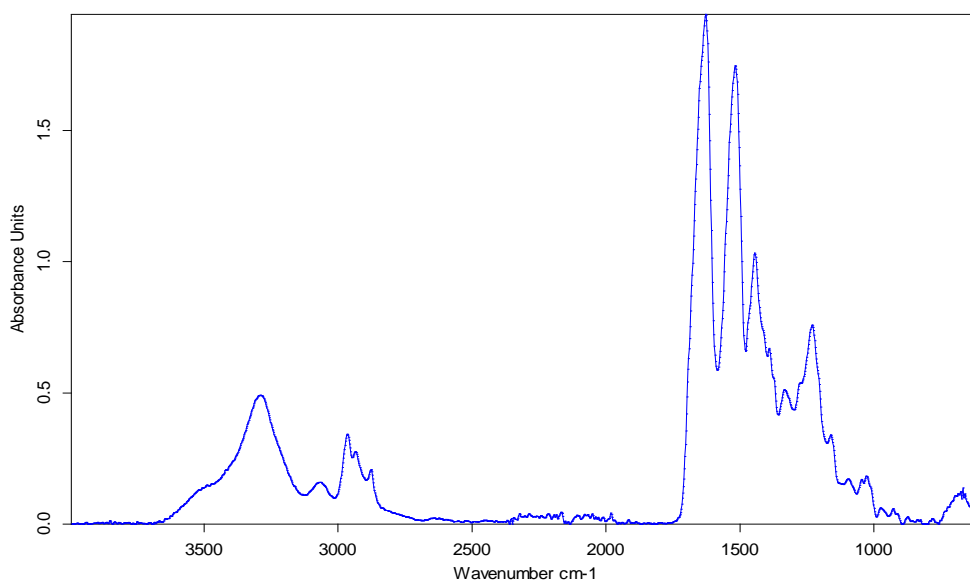
Fig. 17. FTIR of the lyophilized SELR-EGFP.

3.2.4 *Determination of the Inverse Temperature Transition (ITT) by Differential Scanning Calorimetry (DSC) as a function of pH and solvent*

Inverse Temperature Transition (ITT) can be determined by Differential Scanning Calorimetry (DSC) a technique described elsewhere [41]. Briefly, a sample is introduced in an aluminium standard crucible (Mettler Toledo) and placed in the DSC instrument, together with a reference that contains the solvent in which the sample was dissolved. Both are heated at the desired rate and kept at the same temperature. The sample will suffer an endothermic phase transition above its transition temperature which means that a fraction of the heat will be absorbed in this transition, so an additional heat will be necessary to maintain the sample at the same temperature than the reference. The temperature at this point is termed ITT being the lowest value of the observed peak (Fig. 18).
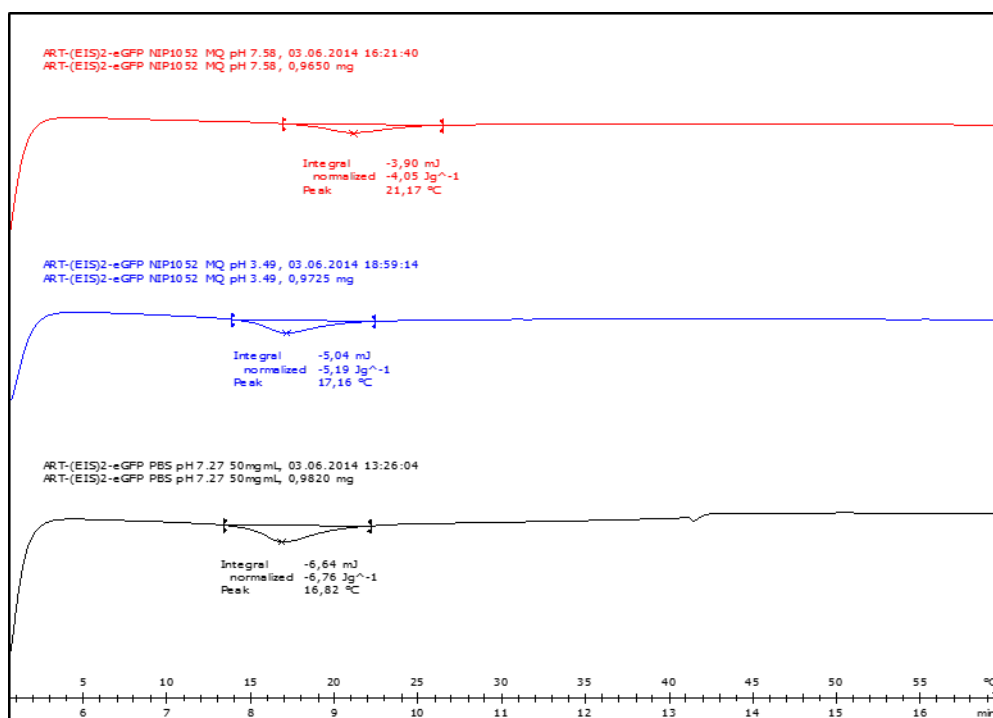
32

Fig. 18. DSC thermogram of SELR-EGFP at different conditions of pH and solvent.

As expected, the ITT is lower in the case of solution of SELR-EGFP in ultrapure water (MilliQ, MQ) at pH 3.49 than when at pH 7.58. This is due to the fact that at pH below the pKa of carboxylic acid (COOH) of glutamic acid residues in the elastin polypeptide chain, i.e. pH 3.49, this group is uncharged (COOH), lowering the interaction with water molecules. This means that there are less water molecules surrounding the protein and therefore a lower temperature or energy is needed in order to break these interactions and promote transition when compared with the SELR-EGFP solution at pH 7.58, because in this case, carboxylic group is deprotonated (COO$^-$) and hence the interaction with water molecules is higher than in the other case.

In PBS, there are different salts present in the solution, which lower the ITT independently of the pH that is buffered neutral (approximately 7), which is very likely to happen in this conditions as described elsewhere..

3.2.5 *Amino acid analysis (HPLC)*

HPLC was performed by an external service in order to assure the amino acid composition. Results are showed in Table 6. In conclusion, experimental results are close to the predicted, differences being explained because of the technique sensitivity.

AMINO ACID	THEORETICAL	EXPERIMENTAL
Alanine	50	50.55
Arginine	6	7.49
Asparagine	14	21.53
Aspartic Acid	18	
Cysteine	2	-
Glutamine	7	49
Glutamic Acid	38	
Glycine	524	562.18
Histidine	9	6.3
Isoleucine	133	136.07
Leucine	21	18.91
Lysine	18	13.68
Methionine	8	7.63
Phenylalanine	12	8.44
Proline	231	231.93
Serine	31	24.74
Threonine	18	11.66
Tryptophan	1	-
Tyrosine	11	8.68
Valine	321	329.23

Table 6. Amino acid composition of the SELR-EGFP calculated by HPLC.

3.3 Evaluation of the fluorescence and nanoparticle formation of (EIS)₂-EGFP as recombinamer intrinsic properties

3.3.1 Evaluation of the fluorescence of an SELR-EGFP solution in different conditions by fluorescence spectroscopy and qualitatively by UV light radiation

Fluorescence intensity was measured in a plate reader, fixing the excitation wavelength in 488 nm and the emission in 530 nm, at different pH values and SELR concentrations to determine the effect of this factors in the fluorescence emission of EGFP. Temperature was fixed at 37ºC.

The data obtained (Fig. 19 and Fig. 20) is in good agreement with the information found in the bibliography concerning EGFP that concludes the fluorescence intensity dependence on pH and on protein concentration. This complying between our data and previous data suggests that the fusion of the EGFP protein to an SELR backbone does not have a disadvantageous effect on the EGFP folding, allowing it to get its native, and subsequently fluorescent, conformation.

Blank is either PBS or MQ, depending on the solvent used to prepare solutions. Experiment was performed at physiological temperature, 37ºC, which is above ITT, so nanoparticles are present in the suspension as determined by DLS at every condition.
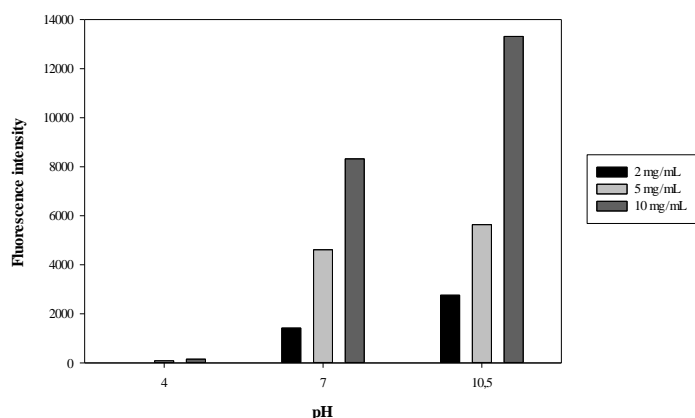

Fig. 19. Fluorescence intensity of SELR-EGFP suspension in ultrapure water (MQ) at different pH and recombinamer concentrations at 37°C.
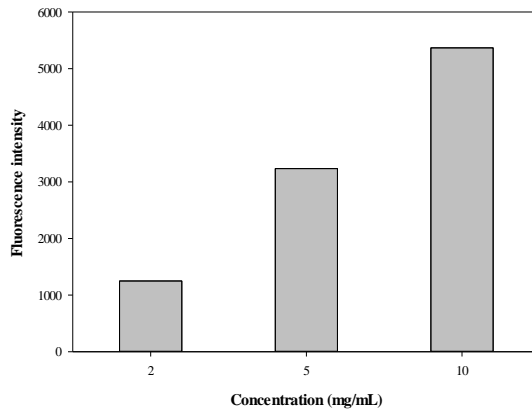
Fig. 20. Fluorescence intensity of SELR-EGFP suspension in PBS at different recombinamer concentrations at 37°C.

With the purpose of confirming fluorescence by actual visualization of this phenomenon, and establish a visual correlation between fluorescence intensity and pH and SELR-EGFP concentration, a photograph of the same plate used to obtain the results in the plate reader showed above was taken (Fig. 21). To observe fluorescence, an ultraviolet lamp to excite the dissimilar samples was needed.
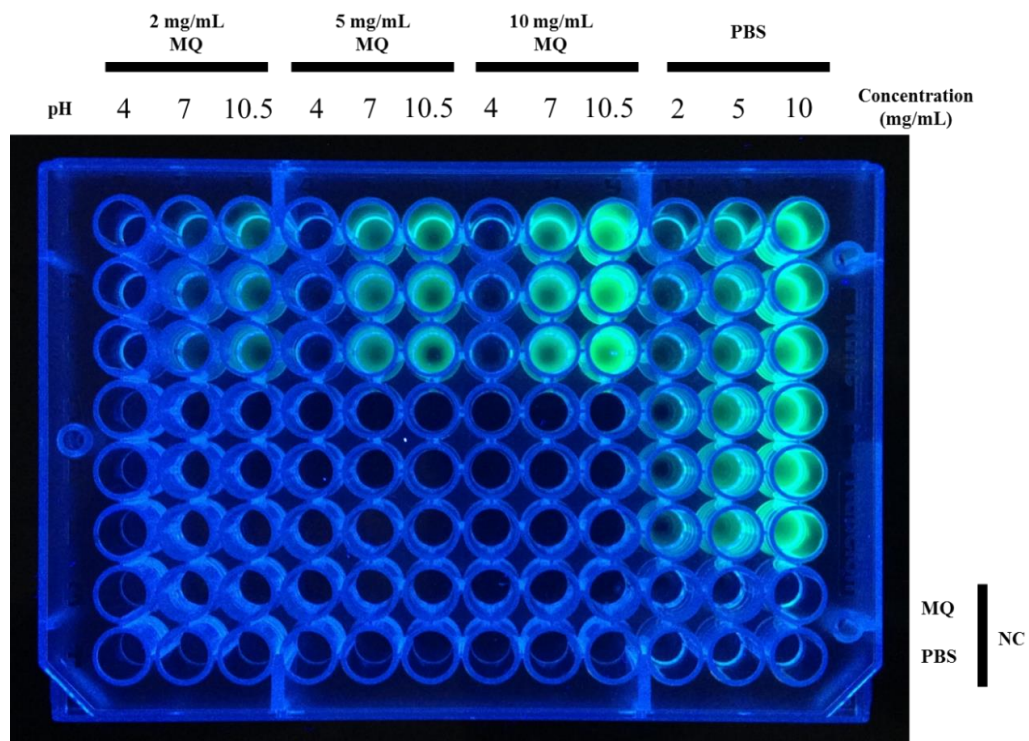

Fig. 21. Picture SELR-EGFP suspension excited with an UV lamp in different solvents, pH and concentrations.

This qualitative result is clearly in concordance with the quantitative ones acquired in the plate reader instrument.

Finally, both types of experiments, qualitative and quantitative give us evidence of fluorescence intensity dependence on SELR-EGFP concentration and pH, as reported elsewhere [27, 29], being a pH of 10.5 and higher recombinamer concentrations the best candidates for a greater fluorescence intensity. Furthermore, there are also slight but clear differences between solvents at the same neutral pH, being more evident when analysing the quantitative results.

3.3.2   Assessment of the SELR-EGFP nanoparticle formation by Dynamic light scattering (DLS) and Transmission Electron Microscopy (TEM)

Dynamic light scattering studies were performed at low concentrations of $(E_{50}I_{60}Silk)_2$-EGFP in order to assess the size of the self-assembled structures derived from the amphiphilic behaviour of the designed SELR [42, 43]. Experiments were carried out at different concentrations of SELR-EGFP solution in different solvents (PBS and ultrapure water). In the case of the SELR dissolved in water, different pH values were used to study the effect of this parameter on the SELR solution at 10 mg/mL.

Size is showed as a distribution where the population of NPs for each size is given by the % of volume. This data is directly linked to the intensity of scattered light by using the formula of a sphere volume, taking into account that the nanoparticles' shape is close to this geometry. %Volume gives more accurate values when several populations are present in the suspension, as intensity is proportional to the size of the particles (for a higher size, higher intensity) and populations of large particles could mask the importance of smaller ones .

All experiments were performed at 37ºC, as mentioned in 2.2.15.1. Polydispersity indexes were all close to 0.2 in every case.

In Fig. 22, size distributions of different concentration suspensions in ultrapure water are shown. Two populations for 5 and 2 mg/mL while for 10 mg/mL only a clear distribution can be observed being a more homogeneous suspension. Size of the main

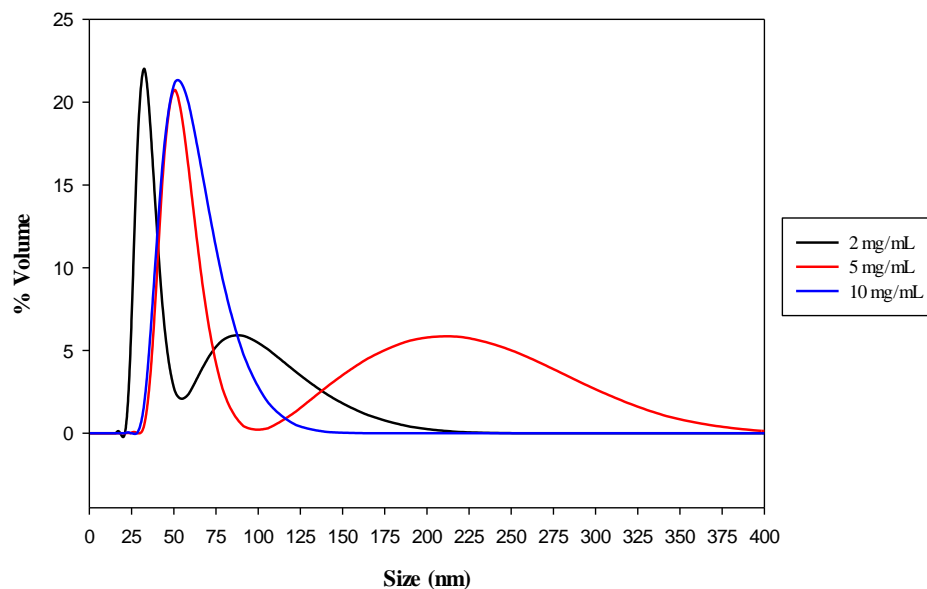distribution is quite similar for 5 and 10 mg/mL, but smaller particles show up for the case of 2 mg/mL.

Fig. 22. Size of (EIS)2-EGFP particles in MQ at different concentrations at pH 7.0.

Fig. 23 shows differences between samples of different concentrations dissolved in PBS (pH 7.2). In this case, a different scenario than when dissolved in MQ takes place, as now 2 mg/mL suspension is the one that arises to a higher size distribution and larger particles than in MQ, while the other two behave contrary, suggesting an effect of salts present on PBS buffer on SELR-EGFP self-assembling into nanoparticles.
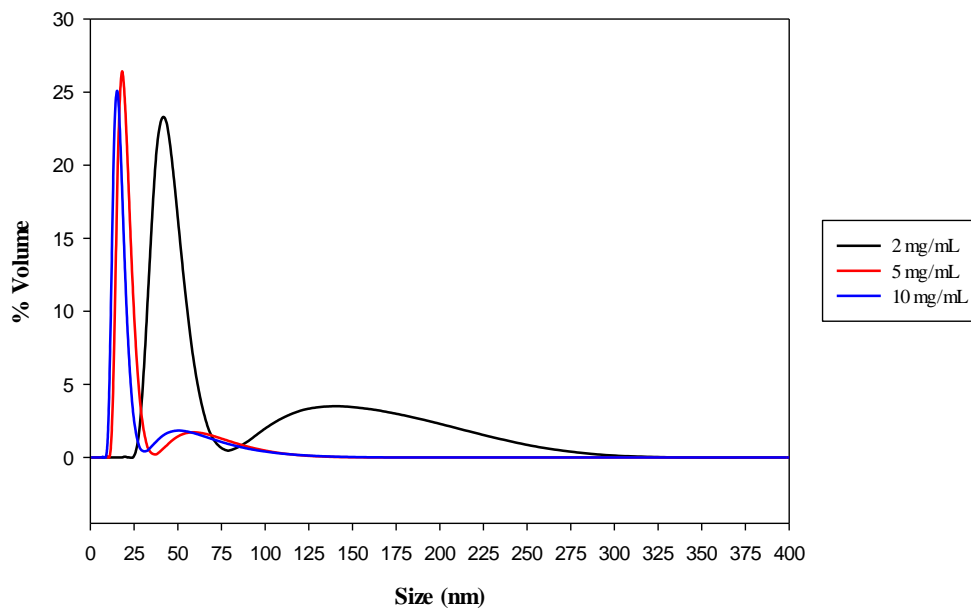
Fig. 23. Size of (EIS)2-EGFP particles in PBS at different concentrations at pH 7.2.

A final experiment was done at 10 mg/mL to assess the effect of pH on the self-assembling, that is, in the size of the obtained nanoparticles. As seen in Fig. 24, there was a tendency to reduce the size of the particle as pH was increased, signifying that pH has any effect on these nanostructures, which is consistent with the fact that there are COOH groups in the SELR fragment and other groups in different residues of the EGFP part, that is a protein of a great heterogeneity of amino acids, that are susceptible of being affected by the pH of the solution. Furthermore, dispersity of the suspension seems to reduce by the increasing of the pH giving narrower distributions.
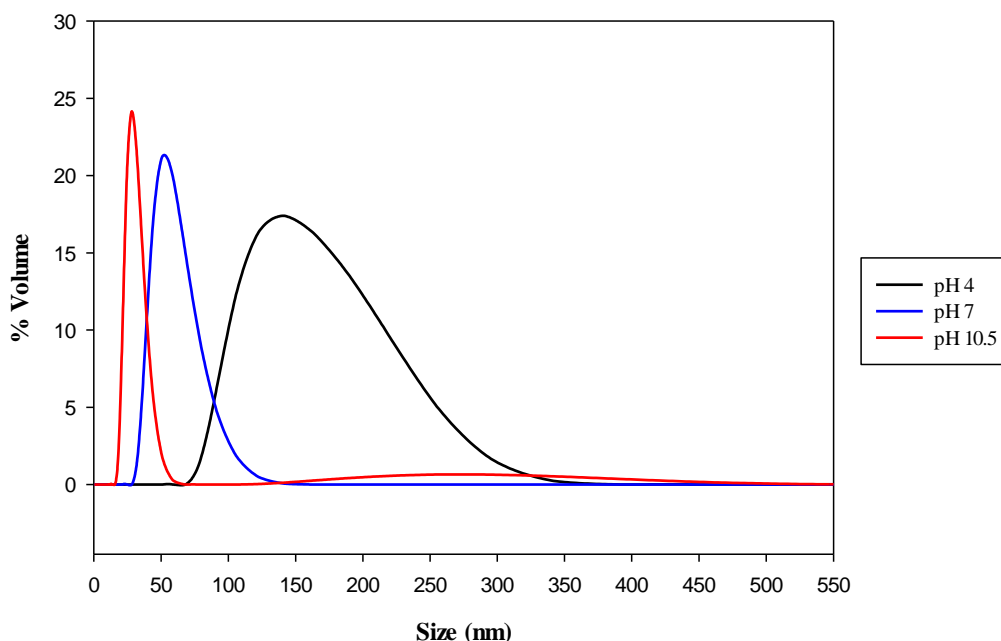
Fig. 24. Size of (EIS)2-EGFP particles at 10 mg/mL in MQ at different pH values.

In conclusion, the size (EIS)$_2$-EGFP nanoparticles is affected by different factors like solvent composition and pH, which is in good agreement with data found elsewhere. Furthermore, concentration of the SELR has an influence on the final size distribution of the nanoparticles. All these factors determine the self-assembling of the SELR-EGFP molecules by having a direct effect either on the material or in the solvent.

With the purpose of effectively observe the formed nanoparticles, a visualization by TEM was performed with the specifications exposed above (2.2.16.3). Different nanoparticles can be seen (Fig. 25), with a range of sizes from less than 25 nm to almost 50 nm, corroborating the polydispersity of the size distribution obtained by DLS.
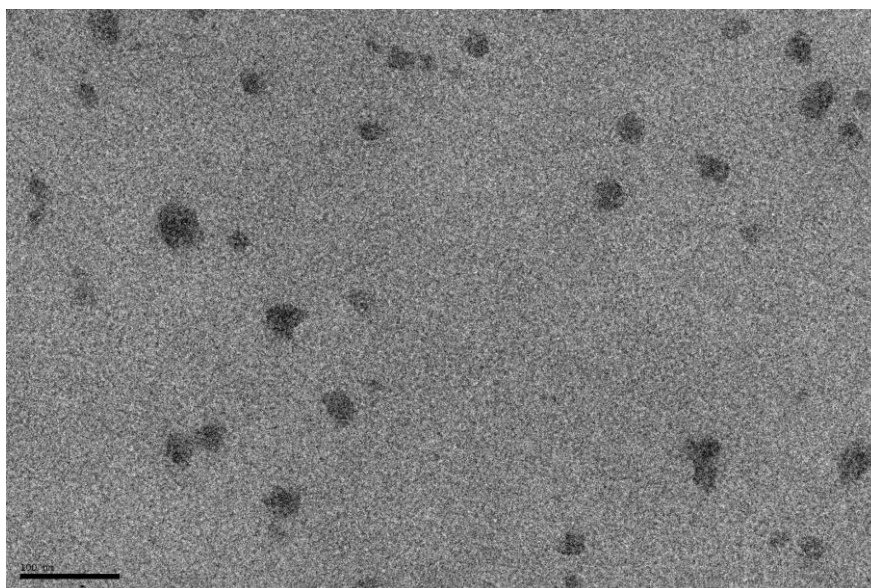
Fig. 25. TEM photograph of a (EIS)2-EGFP nanoparticle suspension at 10 mg/mL in PBS.

3.4 Development of Layer by Layer nanotechnological approach for the obtaining of fluorescent cell adhesive nanopartibles

The nanoparticle structures found by DLS studies of $(E_{50}I_{60}Silk)_2$-EGFP led us to the development of a new hypothesis in order to achieve coated nanoparticles (NPs) by the combination of positively and negatively charged molecules. Although previous work has been done regarding LbL particle formation with ELRs [44], due to the nanoparticle formation without the addition of any mould, the LbL technique is in this case simplified when compared to other traditional LbL approaches: by the simple heating at 37ºC of the $(E_{50}I_{60}Silk)_2$-EGFP solution, more or less stable nanoparticles are obtained. Then, an ELR with positively charged groups called HRGD6 is added to the suspension and NPs become coated by electrostatic interactions. This ELR confers the ability of promote cell adhesion through integrins present in the cell membrane by the RGD amino acid sequences present in this protein. Furthermore, if a positive and stable charge is achieved, NPs could be internalized by cells when added to a cell culture.

Because of the probable possibility of nano and microparticle aggregation during LbL process if higher than 1mg/mL concentrations were used, in this case lower concentrations than the studied above were chosen: 1, 0.5 and 0.2 mg/mL of final

41

concentration of (EIS)$_2$-EGFP taking into account the volume needed to add of HRGD6 recombinamer solution. Procedure is described in materials and methods section.

3.4.1   Zeta potential and size measurements

To analyse the particle behaviour, zeta potential measurement studies were carried out at different concentrations of (E$_{50}$I$_{60}$Silk)$_2$-EGFP and afterwards in different ratios of NH$_3^+$: COO$^-$ (from the side chains of lysine from HRGD6 and glutamic acid from (E$_{50}$I$_{60}$Silk)$_2$-EGFP, respectively). Experiments were performed at human physiological temperature (37ºC). First results can be seen in Table 7 and Table 8.

[(EIS)2-EGFP] (mg/mL)	Z-Potential (mV)	Size (nm)
0.2	-34.87	110
0.5	-38.03	150
1	-33.27	185

Table 7. Inital size and zeta potential measurements of SELR-EGFP at different concentrations.

[(EIS)$_2$-EGFP] (mg/mL)	NH$_3^+$:COO$^-$ molar ratio	Z-Potential (mV)	Size (nm)
0.2	1:1	-26.67	151
	2:1	-25.1	160
	5:1	-14.3	370

Table 8. Zeta potential and size of different NH$_3^+$:COO$^-$ ratios at a single concentration as a proof-of-concept LbL experiment.

Initially, three different ratios were chosen, as seen above. By the measurement of a single concentration of every ratio, all of them were discarded, as they weren't suitable for the achievement of nano and microparticles capable of being internalized by cells, since they are supposedly needed to be positively charged. Even though, an increase in size of the particles while increasing the ratio can be perceived, suggesting two possibilities: an actual increase in the microns scale or an

aggregation. Observing the particle suspension of 5:1 ratio, there is obvious evidence of macroparticles formation (data not shown). This is not a desired phenomenon, but this problem could not be resolved neither by strong stirring nor by changing the temperature of the layer by layer process, always above the Tt of SELR-EGFP.

As a 5:1 ratio of NH_3^+:COO^- was insufficient to achieve positively charged particles, higher ratios were used. However, this ratio was still used for further experiments at higher concentrations to see if any effect related to this parameter occurs. The lowest SELR-EGFP concentration of 0.2 mg/mL was also discarded as the suspension of this particles was barely detected as fluorescent in a plate reader (data not shown). A summary of the results in size and zeta potential measurements of 0.5 and 1 mg/mL can be seen in Table 9.

[(EIS)$_2$-EGFP] (mg/mL)	NH_3^+:COO^- molar ratio	Z-Potential (mV)	Size (nm)
0.5	5:1	12.27	530
	10:1	13.47	602
1	5:1	11.63	550
	10:1	12.33	756

Table 9. Zeta potential and size values for the different combinations of concentrations and ratios

Surprisingly, at 0.5 and 1 mg/mL a ratio of 5:1 was enough to achieve positively charged nanoparticles when it did not happen for the 0.2 mg/mL suspension, maybe due to the HRGD6 cross-linking between nanoparticles, leading to an aggregation and not stable nor homogeneous particles. Nevertheless, molar ratio of 10:1 was not rejected in order to see experimental differences between both ratios in cell culture experiments.

With the aim of getting more stable and less disperse nanoparticles by the continuous increase in the hydrophobic interactions between silk domains, (EIS)$_2$-EGFP suspensions were incubated for 1 week at 37ºC prior to LbL approach and data at different times of incubation of size and zeta potential were recorded (Table 10). Finally, these suspensions were used for LbL and successively in cell culture experiments, although no improvement in the stability nor in the polydispersity of the

suspension could be detected. In this study, initial SELR-EGFP concentration is studied, that is, the recombinamer concentration before the addition of HRGD6 solution (0.625 and 1.67 mg/mL for 0.5 and 1 mg/mL, respectively).

[(EIS)$_2$-EGFP] (mg/mL)	Time (days)	Z-Potential (mV)	Size (nm)
0.625	1	-31.56	160
	3	-30.43	155
	7	-31.89	156
1.67	1	-29.07	192
	3	-29.85	194
	7	-30.91	197

Table 10. Zeta potential and size measurements at different incubation times and concentrations of SELR-EGFP

The fact that size stabilization is not being achieved by an increasing in the incubation time, nor polydispersity is lowering could be explained by the fibre arrangement of the recombinamer, leading to a more complex structure that cannot be completely described by DLS. Hence, further characterization should be done by different methods, such as atomic force microscopy (AFM) and/or transmission electron microscopy (TEM).

3.4.2 Cell culture of LbL nanoparticles

HFF-1 cell line (fibroblasts) was used to perform the cell adhesion and/or internalization experiment, as is a very common line in the study of the adhesion properties of materials. Procedure is described in Materials and Methods section.

Phase contrast and fluorescence microscope coupled to a camera was used to take pictures of the different culture conditions at different times. At time 2 hours after the addition of culture medium supplemented with either 1 mg/mL or 0.5 mg/mL suspension, only in the first case particles could be seen, probably because the higher amount present in this suspension and the higher probability of sedimentation in that short time period (Fig. 26). Silk-elastin-like recombinamer nanoparticles are ordered randomly probably just by simple precipitation. There is no full evidence at this time

that particles are adhered to cell surface and not just deposited, so further investigations were done at 24 hours.
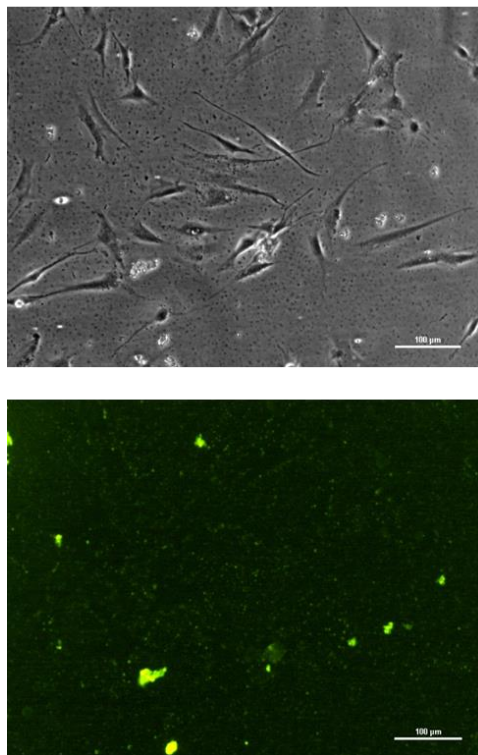
1mg/mL ELR-EGFP LbL 2 hours

Fig. 26. HFF-1 cell culture in DMEM medium supplemented with 1 mg/mL suspension of SELR-EGFP nanoparticles covered with HRGD6 by LbL after 2 hours of incubation. Phase contrast (up) and fluorescence (down) microscopy photographs of the same area.

After 24 hours of cell culture, pictures were taken in order to assess the development of the nanoparticles and if cell adhesion or even internalization could be demonstrated. Although more precise experiments should be performed, this observation could also lead to the verification of cytotoxicity of the SELR nanoparticles.

In Fig. 26, it can be observed how SELR nanoparticles from a 1 mg/mL suspension are preferentially arranged on cell surface, while areas corresponding to the bottom of the well are emptier, suggesting an evolution during time of the cells and nanoparticles to meet themselves by the comparison of the photographs in this figure with the ones in Fig. 27. Internalization cannot be discarded since green fluorescence can be observed through all the cell cytoplasm. In the case of the medium

supplemented with 0.5 mg/mL nanoparticles, it can be seen the lesser number of NPs than in the other case, and a more aggregated state, but still a preferable arrangement on cell surface, being even more clear the non-presence of the NPs on the areas of well without cells.
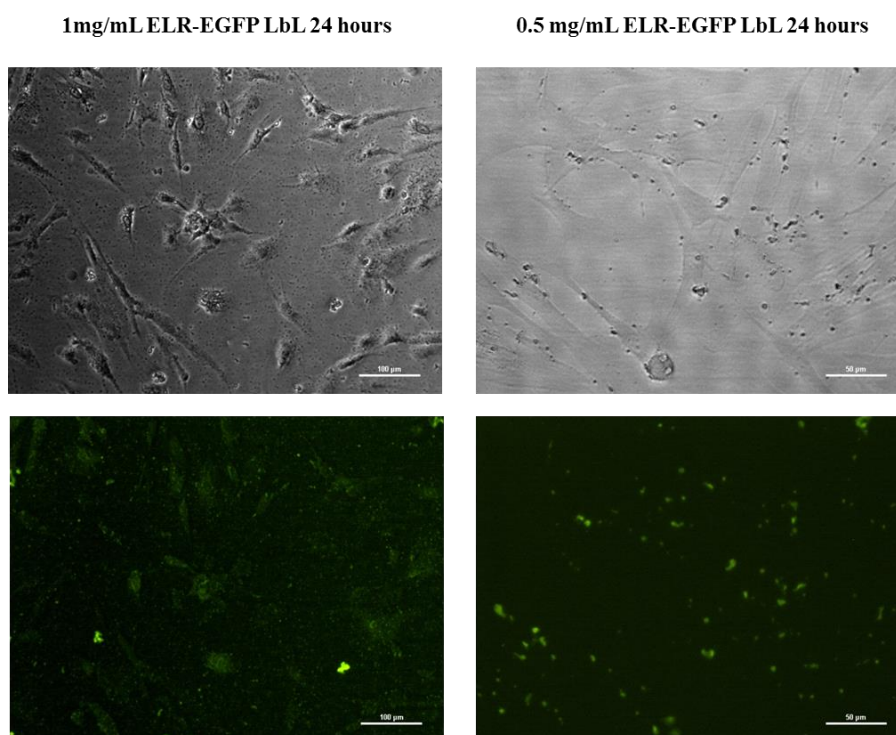

Fig. 27. HFF-1 cell culture in DMEM medium supplemented with 1 and 0.5 mg/mL suspension of SELR-EGFP nanoparticles covered with HRGD6 by LbL after 24 hours of incubation. Phase contrast (up) and fluorescence (down) microscopy photographs of the same area.

With the information displayed above, it is not really clear if NPs are on the surface or in the cell cytoplasm. To discern between these two possibilities, another picture (Fig. 28) was taken with another focus in order to visualize the cell surface. Shining points refer to SELR nanoparticles and this brilliance, meaning that NPs are reflecting light, suggests that nanoparticles are not internalized but adhered on cell surface. However, it should be studied thoroughly in future studies by the combination of more precise techniques, like visualization in a confocal microscope.
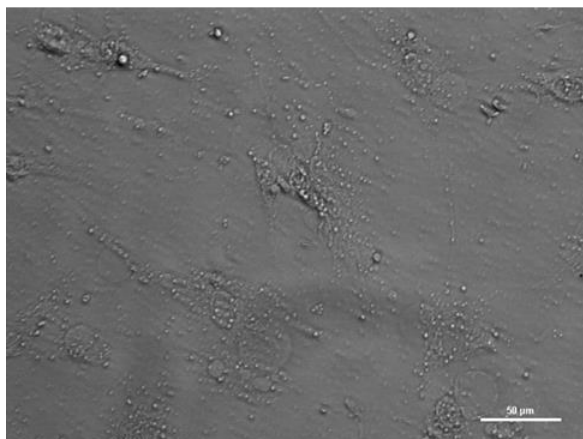
1mg/mL ELR-EGFP LbL 24 hours

Fig. 28. HFF-1 cell culture in DMEM medium supplemented with 1 mg/mL SELR nanoparticles suspension after 24h of incubation. Focus set at cell surface.

3.5   Qualitative examination of the fluorescent hydrogel

As described in 1.2.2 and 3.1, (EIS)$_2$-EGFP recombinamer has the ability of collapsing when dissolved at high concentrations in an aqueous solvent, which leads to the formation of an hydrogel structure.

To qualitatively assess the gelification process and the fluorescence of the recombinamer hydrogel, two solutions of SELR-EGFP at 150 mg/mL were prepared, the first one using ultrapure water (MQ) as solvent and the other one using PBS as a physiological buffer standard. When dissolved, solutions were place at 37ºC for 1 hour and 1 day and pictures were taken to study the gel formation and the intrinsic fluorescence of the material.

As it can be observed in Fig. 29, hydrogels were stable in both cases at 30 minutes and 24 hours of incubation, suggesting that the gelification process is fast, probably only few minutes needed after incubation at a temperature above Tt for stable gel formation. Hydrogel kinetics should be studied by other more accurate and quantitative techniques such as rheology.
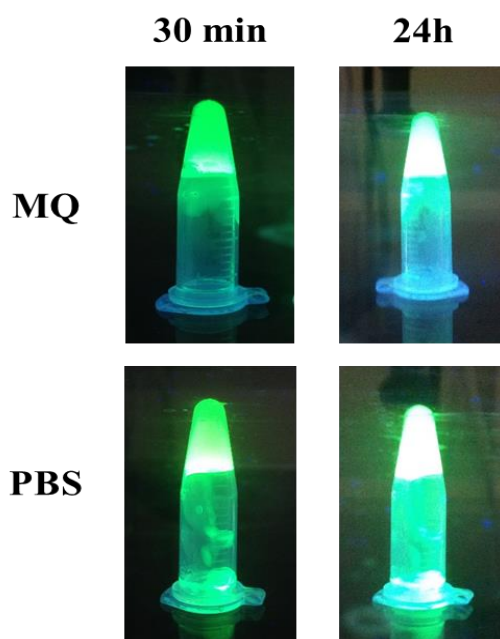
Fig. 29. Qualitative examination of fluorescence and stability of SELR-EGFP hydrogels either in ultrapure water (MQ) or in PBS after different times of incubation at 37ºC. UV transilluminator used as excitation source.

Regarding fluorescence, this same figure shows that fluorescence is evident in these conditions, confirming that there is no influence of the folding of the silk-elastin-like backbone on EGFP folding, even when other structures different from nanoparticles are formed. In addition, and in agreement with the findings showed above, hydrogels are fluorescent both as when SELR-EGFP dissolved in ultrapure water and when in PBS. The observed fluorescence intensity differences are due to an artefact of the photography system used to take pictures and not to a change in this parameter along the time.

4. CONCLUSIONS

The increasing knowledge of phenomena in the nanometre scale is leading to the development of different tools in diverse fields by a set of approaches closely related to chemistry and physics. In this way, biological systems are also susceptible of being considered nanotechnological tools since, in many cases, processes such as self-assembling are spontaneous in nature implying different kinds of biomolecules, including proteins like human elastin.

By the recombinant DNA technology it is able to design and produce in *E.coli* host different proteins like elastin derivatives, named elastin-like recombinamers (ELRs), in order to achieve a biomaterial with very controlled self-assembling properties depending on ELRs composition.. It is also possible to fuse other bioactive peptides or proteins to these recombinamers to improve its functionalities and the combination with other molecules with self-assembly properties, like silk domains derive from silk of *Bombyx mori*.

The Enhanced Green Fluorescent Protein has been widely used during the last decades in molecular biology applications and has very promising uses in the development of biomedical devices for imaging purposes. By these means, an SELR-EGFP fusion protein was designed, produced and characterize in order to determine the properties of this material.

It was also achieved dual bioactive particles with self-assembling capacity as much as fluorescence emission and cell adhesion by the RGD sequence of the second recombinamer. These particles were capable of adhering to the cell surface and even of internalization, although this phenomenon it is not really clear with the information presented above and should be thoroughly studied with other techniques such as visualization with a confocal microscope, which allows a very good observation through every level of the cells.

In conclusion, this work it is just a starting point for further characterization of the material, especially regarding the size of the nanoparticles and the evaluation of fibre formation in different conditions and the potential application of SELR-EGFP

hydrogels in biomedicine to track implants through the body. There is also plenty of space for the improvement of the methods developed during the experiments performed considering that most of them were carried out just once and/or with some time limitations. For example, controls using the SELR used as a backbone of the final fluorescent recombinamer should be included in following works, mainly studies of particle size and z-potential characterization as the influence of EGFP on the self-assembling process has not been addressed. There is also need to perform further visualization experiments to evaluate if exists or not internalization of the layer by layer resulting nanoparticles and, if not, it should be pursued by the changing of charge ratios as it could have some potential applications for *in vitro* and *in vivo* studies.

As a final remark regarding hydrogels, *in vivo* tests could be very useful to determine if this material can be well tracked when injected or implanted in an organism. Besides, mechanical properties should be evaluated by rheology at different concentrations of either single SELR-EGFP hydrogels or a combination of different hydrogel forming ELRs with other suitable bioactivities.

REFERENCES

[1] Hu X, Cebe P, Weiss AS, Omenetto F, Kaplan DL. Protein-based composite materials. Materials Today 2012;15:208-15.

[2] A G, A F-C, IM L, JC R-C, FJ A. - Elastin-like recombinamers: biosynthetic strategies and biotechnological. D - 101265833:- 1174-86.

[3] Rodriguez-Cabello JC, Girotti A, Ribeiro A, Arias FJ. Synthesis of genetically engineered protein polymers (recombinamers) as an example of advanced self-assembled smart materials. Methods in molecular biology 2012;811:17-38.

[4] MacEwan SR, Chilkoti A. Elastin-like polypeptides: biomedical applications of tunable biopolymers. Biopolymers 2010;94:60-77.

[5] Rodríguez-Cabello JC, Martín L, Alonso M, Arias FJ, Testera AM. "Recombinamers" as advanced materials for the post-oil age. Polymer 2009;50:5159-69.

[6] Mithieux SM, Weiss AS. Elastin. Advances in protein chemistry 2005;70:437-61.

[7] Debelle L, Tamburro AM. Elastin: molecular description and function. The international journal of biochemistry & cell biology 1999;31:261-72.

[8] Miao M, Bellingham CM, Stahl RJ, Sitarz EE, Lane CJ, Keeley FW. Sequence and structure determinants for the self-aggregation of recombinant polypeptides modeled after human elastin. The Journal of biological chemistry 2003;278:48553-62.

[9] Di Zio K, Tirrell DA. Mechanical Properties of Artificial Protein Matrices Engineered for Control of Cell and Tissue Behavior. Macromolecules 2003;36:1553-8.

[10] Rodríguez-Cabello JC, Reguera J, Girotti A, Arias FJ, Alonso M. Genetic Engineering of Protein-Based Polymers: The Example of Elastinlike Polymers. Advances in Polymer Science 2006;200:119-67.

[11] Urry DW. What sustains life? Consilient mechanisms for protein-based machines and materials. New York: Springer-Verlag; 2006.

[12] B V, AS W. - Biochemistry of tropoelastin. D - 0107600:- 1-18.

[13] Uitto J. Biochemistry of the Elastic Fibers in Normal Connective Tissues and its Alterations in Diseases. J Investig Dermatol 1979;72:1-10.

[14] Urry DW, Hugel T, Seitz M, Gaub HE, Sheiba L, Dea J, et al. Elastin: a representative ideal protein elastomer. Philosophical transactions of the Royal Society of London Series B, Biological sciences 2002;357:169-84.

[15] Cox BA, Starcher BC, Urry DW. Coacervation of alpha-elastin results in fiber formation. Biochimica et biophysica acta 1973;317:209-13.

[16] Urry DW. Physical Chemistry of Biological Free Energy Transduction As Demonstrated by Elastic Protein-Based Polymers†. The Journal of Physical Chemistry B 1997;101:11007-28.

[17] Duncan R. The dawning era of polymer therapeutics. Nature reviews Drug discovery 2003;2:347-60.

[18] Smart T, Lomas H, Massignani M, Flores-Merino MV, Perez LR, Battaglia G. Block copolymer nanostructures. Nano Today 2008;3:38-46.

[19] Huang L, McMillan RA, Apkarian RP, Pourdeyhimi B, Conticello VP, Chaikof EL. Generation of Synthetic Elastin-Mimetic Small Diameter Fibers and Fiber Networks. Macromolecules 2000;33:2989-97.

[20] Lee TAT, Cooper A, Apkarian RP, Conticello VP. Thermo-Reversible Self-Assembly of Nanoparticles Derived from Elastin-Mimetic Polypeptides. Advanced Materials 2000;12:1105-10.

[21] Rodriguez-Cabello JC, Martin L, Girotti A, Garcia-Arevalo C, Arias FJ, Alonso M. Emerging applications of multifunctional elastin-like recombinamers. Nanomedicine 2011;6:111-22.

[22] Kundu B, Rajkhowa R, Kundu SC, Wang X. Silk fibroin biomaterials for tissue regenerations. Advanced drug delivery reviews 2013;65:457-70.

[23] Megeed Z, Cappello J, Ghandehari H. Genetically engineered silk-elastinlike protein polymers for controlled drug delivery. Advanced drug delivery reviews 2002;54:1075-91.

[24] Dandu R, Cresce AV, Briber R, Dowell P, Cappello J, Ghandehari H. Silk–elastinlike protein polymer hydrogels: Influence of monomer sequence on physicochemical properties. Polymer 2009;50:366-74.

[25] Qiu W, Teng W, Cappello J, Wu X. Wet-Spinning of Recombinant Silk-Elastin-Like Protein Polymer Fibers with High Tensile Strength and High Deformability. Biomacromolecules 2009;10:602-8.

[26] Shimomura O, Johnson FH, Saiga Y. Extraction, purification and properties of aequorin, a bioluminescent protein from the luminous hydromedusan, Aequorea. Journal of cellular and comparative physiology 1962;59:223-39.

[27] Campbell TC, F. The effect of pH on Green Fluorescent Protein: A Brief Review. Molecular Biology Today 2001;2:1-4.

[28] Tsien RY. The green fluorescent protein. Annual review of biochemistry 1998;67:509-44.

[29] Haupts U, Maiti S, Schwille P, Webb WW. Dynamics of fluorescence fluctuations in green fluorescent protein observed by fluorescence correlation spectroscopy. Proceedings of the National Academy of Sciences 1998;95:13573-8.

[30] AS HPV. GFP sensors. Advanced Concepts in Fluorescence Sensing 2005;Part B: Macromolecular Sensing.

[31] Rao J, Dragulescu-Andrasi A, Yao H. Fluorescence imaging in vivo: recent advances. Current opinion in biotechnology 2007;18:17-25.

[32] Wolenski JS, Julich D. Fluorescence microscopy gets faster and clearer: roles of photochemistry and selective illumination. The Yale journal of biology and medicine 2014;87:21-32.

[33] Weigert R, Porat-Shliom N, Amornphimoltham P. Imaging cell biology in live animals: ready for prime time. The Journal of cell biology 2013;201:969-79.

[34] Yang F, Moss LG, Phillips GN, Jr. The molecular structure of green fluorescent protein. Nature biotechnology 1996;14:1246-51.

[35] Cormack BP, Valdivia RH, Falkow S. FACS-optimized mutants of the green fluorescent protein (GFP). Gene 1996;173:33-8.

[36] Chung CT, Niemela SL, Miller RH. One-step preparation of competent Escherichia coli: transformation and storage of bacterial cells in the same solution. Proceedings of the National Academy of Sciences of the United States of America 1989;86:2172-5.

[37] Laemmli UK. Cleavage of structural proteins during the assembly of the head of bacteriophage T4. Nature 1970;227:680-5.

[38] Lee C, Levin A, Branton D. Copper staining: a five-minute protein stain for sodium dodecyl sulfate-polyacrylamide gels. Analytical biochemistry 1987;166:308-12.

[39] Martin L, Arias FJ, Alonso M, Garcia-Arevalo C, Rodriguez-Cabello JC. Rapid micropatterning by temperature-triggered reversible gelation of a recombinant smart elastin-like tetrablock-copolymer. Soft Matter 2010;6:1121-4.

[40] Barth A. Infrared spectroscopy of proteins. Biochimica et biophysica acta 2007;1767:1073-101.

[41] Ribeiro A, Arias FJ, Reguera J, Alonso M, Rodríguez-Cabello JC. Influence of the Amino-Acid Sequence on the Inverse Temperature Transition of Elastin-Like Polymers. Biophysical Journal;97:312-20.

[42] Martín L, Castro E, Ribeiro A, Alonso M, Rodríguez-Cabello JC. Temperature-Triggered Self-Assembly of Elastin-Like Block Co-Recombinamers:The Controlled Formation of Micelles and Vesicles in an Aqueous Medium. Biomacromolecules 2012;13:293-8.

[43] Pinedo-Martín G, Castro E, Martín L, Alonso M, Rodríguez-Cabello JC. Effect of Surfactants on the Self-Assembly of a Model Elastin-like Block Corecombinamer: From Micelles to an Aqueous Two-Phase System. Langmuir 2014;30:3432-40.

[44] Costa RR, Testera AM, Arias FJ, Rodríguez-Cabello JC, Mano JF. Layer-by-Layer Film Growth Using Polysaccharides and Recombinant Polypeptides: A Combinatorial Approach. The Journal of Physical Chemistry B 2013;117:6839-48.